THE PENNSYLVANIA STATE UNIVERSITY
SCHREYER HONORS COLLEGE

DEPARTMENT OF BIOCHEMISTRY AND MOLECULAR BIOLOGY

DEFINING STAGE-SPECIFIC AND CONSTITUTIVE PROMOTERS IN PLASMODIUM YOELII

LOGAN FINGER
SPRING 2019

A thesis
submitted in partial fulfillment
of the requirements
for a baccalaureate degree in
Biochemistry and Molecular Biology
with honors in Biochemistry and Molecular Biology

Reviewed and approved* by the following:

Scott E. Lindner
Assistant Professor of Biochemistry and Molecular Biology
Thesis Supervisor

Joseph Reese
Professor of Biochemistry and Molecular Biology
Associate Department Head for Research and Faculty Development
Honors Adviser

Wendy Hanna-Rose
Department Head for Biochemistry and Molecular Biology

* Signatures are on file in the Schreyer Honors College

Abstract

Developmentally attenuated malaria parasites have shown to be of interest due to their potential to be live-attenuated vaccine candidates. An increasingly common way to modify parasites so that the effects of essential gene deletions/modifications can be studied is through the use of CRISPR/Cas9.

In this series of experiments, I show through the use of fluorescence microscopy and flow cytometry that HSP70-2/BiP, which is active within all stages of the parasites life cycle, is capable of driving production of green fluorescence protein (GFP) constitutively *in vivo*. In tests comparing different lengths of the BiP promoter, I seek to determine the minimal composition of the promoter can be such that it is still functional. Likewise, these tests help establish what qualifies as the minimal promoter for HSP70-2/BiP. Determining this will help with plasmid construction by diversifying the promoter types used within transgene expression plasmids. By doing this, the number of recombination events that tend to occur during replication of the plasmid within bacteria or within the parasite after transfection can be minimized. Additionally, elucidating a correlation between promoter composition and expression level could be useful in controlling expression levels *in vivo*.

Similarly, through testing different stage-specific promoters using fluorescence microscopy and immunofluorescence assays, I can determine when a given promoter is active throughout the lifecycle of the parasite. This information could be used to transcribe desired transgenes such as the Cas9, protein and sgRNAs to enable the targeting of essential genes at specific stages of the parasite's lifecycle, thereby producing developmentally attenuated parasites capable of infecting a host but with no ability to mature further. If these developmentally arrested parasites were used in a vaccine, they could effectively infect a host but be unable to cause an

infection. Thereby, this would expose the body to parasites against which antibodies and other immune responses could be produced but without the risk of developing the disease. In addition to CRISPR, other genetic tools such as CRE/lox recombination, DiCre recombination, and promoter swap experiments also serve to benefit from stage-specific promoters.

TABLE OF CONTENTS

LIST OF FIGURES

LIST OF TABLES

Acknowledgements

First and foremost, I would like to thank my thesis supervisor Dr. Scott Lindner for supporting my endeavors inside and outside of the laboratory. I appreciate his willingness to serve as a mentor to me for the past two years and for the guidance he has provided throughout the entirety of this thesis project and in my aspirations to attend medical school. Additionally, I must recognize former graduate student and now, post-doctoral fellow Dr. Kevin Hart for his supervision and assistance in all the experiments described and performed in this work. I would also like to thank the current and former members of the Lindner Laboratory for their efforts in making this thesis possible; in particular, Laura Bowman whose work laid the foundation for this project. Furthermore, without the staff of the vivarium who ensured the well-being of my mice throughout the course of my experiments this project would not have been possible. Lastly, I would like to recognize the sources that provided funding for these experiments, including the start-up funds given to Scott Lindner by The Pennsylvania State University and the Eberly College of Science for providing the laboratory with undergraduate research grants.

Chapter 1

Introduction

Malaria is caused by the protozoan parasite *Plasmodium*. In 2016, there were over 200 million cases and 400,000 deaths caused by this parasite[1]. An even more staggering statistic is that of these deaths, 70% of them occurred within the 0 to 5 age group. Therefore, it is crucial that a vaccine or drug be developed to combat this deadly disease. To date, there is only one malaria vaccine that, in Phase 3 clinical trials, has shown to be effective in providing partial resistance within children[2]. As a result, the vaccine has been fully licensed by the World Health Organization and its widespread implementation is planned between 2018 and 2022[3]. However, it has only been shown to be effective 55.8% of the time in children 5-17 months old and only 31.3% of the time in infants 6-12 weeks old[2]. Efficacy was also shown to decrease significantly over time conferring adequate resistance for only about a year following the doses. This highlights the need for the development of other safe, more effective vaccine candidates.

Current scientific work has sought to find drug targets and vaccine candidates through utilizing CRISPR/Cas9 to target essential genes associated with the parasite's development. The goal of this project was to identify and characterize promoter sequences of *Plasmodium* genes to potentially be used to drive Cas9 protein and sgRNAs capable of targeting essential genes within the parasite. This project sought to analyze a select number of promoters used by the parasite during asexual- and sexual-blood stages, early-mosquito stages (day seven oocysts), late-mosquito stages (day 10 midgut sporozoites and day 14 salivary gland sporozoites) and early (24 hour)- and late (48 hour)-liver stages of the life cycle. I characterized promoters that would potentially allow for protein expression at certain points in the parasite's life cycle. For instance,

promoters that drive expression in only one stage of the life cycle could be used to target a gene for disruption by CRISPR/Cas9 in that stage. With the knowledge gained from this work, we will be able to target blood-stage essential genes in the mosquito or liver stage for potential use as a genetically attenuated parasite vaccine.

The *Plasmodium* species has a characteristically complex life cycle that involves a host and a vector (figure 1)[4]. The life cycle of the parasite begins when a mosquito takes a blood meal from the human host, effectively transferring sporozoites into the skin, and then into the bloodstream which is used for passive travel to the liver. In the liver, the sporozoites infect hepatocytes and then asexually develop into liver-stage schizonts. The parasite eventually bursts from the hepatocytes releasing infectious merosomes---packages of merozoites---into the blood where they can invade erythrocytes. In the erythrocytes, the parasite first enters the ring stage, then the trophozoite stage and finally the schizont stage. At the schizont stage, the erythrocytes lyse releasing more merozoites allowing the cycle to continue. Alternatively, the parasite can enter the erythrocyte where it can once again enter the ring stage, but rather than continuing to the trophozoite stage, the parasites differentiate into male or female gametocytes. At this stage of the life cycle, transmission from host to vector can be accomplished when another mosquito takes a blood meal from the infected human. Now that the parasite is in the midgut of the mosquito, male and female gametocytes activate. For males, this process consists of producing and releasing eight gametes, while, for females, they shed the host membrane to expose the female gamete. A male gamete can then penetrate the female gamete to form a zygote. Zygotes then develop into motile ookinetes, which burrow through the midgut wall and develop into oocysts under the basal lamina. The oocysts continue to grow as parasite replication continues until finally, they burst, releasing sporozoites. The sporozoites then migrate through the

hemocoel where they become fully infectious and then actively invade the salivary gland of the mosquito. There they await the next blood meal so that they can infect a new host. This process then repeats itself allowing the parasite to develop and infect many new hosts.

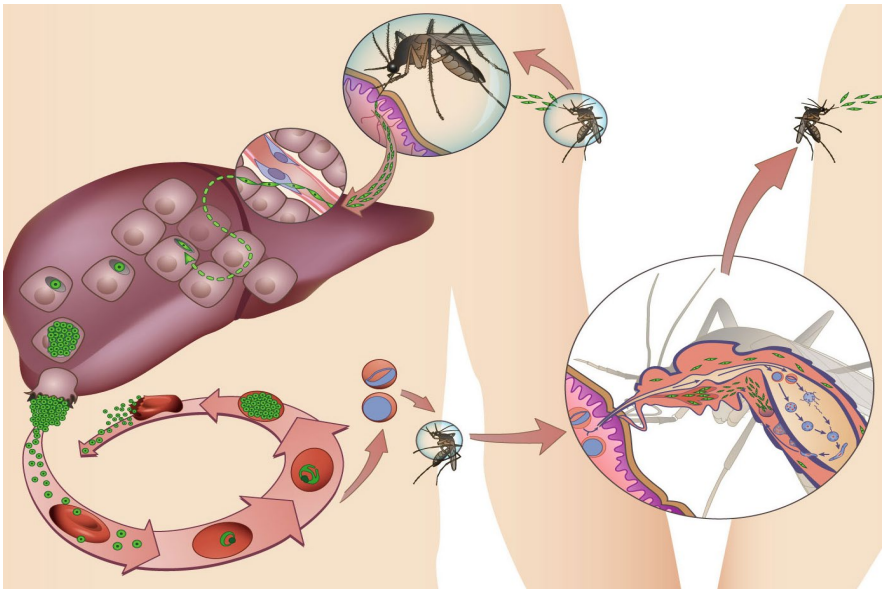

Figure 1. Malaria Parasite's Life Cycle

Figure 1. Malaria Parasite's Life Cycle

During the parasite's progression from stage to stage in its life cycle, different genes are activated or repressed to allow for maturation to occur. Some of these genes are shown to be essential for the development of the parasite and therefore, if they were disrupted or deleted, the parasite would be arrested in a particular stage. This is the basis for a proposed vaccine candidate class, called genetically attenuated parasites (GAPs)[5]. A method for performing this type of gene modification or deletion using the CRISPR/Cas9 system, rather than traditional homologous recombination, has been proposed. CRISPR/Cas9 was first discovered in bacteria and archaea as a means of adaptive immunity for these microorganisms against infecting bacteriophage. CRISPR is so-called because of the clustered regularly interspaced short palindromic repeats within the genome of the archaea or bacteria, which are homologous to regions in the genetic

material contained within the phage. The homology serves as a marker indicating that the foreign genetic material invading the cell is that of a phage and should be destroyed. These CRISPR sequences are derived from the phage DNA when the host cell cuts a portion of the invading DNA out and incorporates it into a region of its own genome known as the CRISPR array. When the CRISPR array is transcribed, other proteins can cut this RNA to produce crRNA, which include the phage-specific targeting sequence. This crRNA, in conjunction with a tracrRNA, which are collectively known as a guide RNA (gRNA), bind the Cas9 protein. The Cas9/gRNA complex then systematically searches the DNA for 1) the proto-spacer adjacent (PAM) motif, 2) the proximal "seed" sequence and finally, 3) the complete target sequence. The Cas protein creates a double-stranded break in the DNA to which it has sufficiently high affinity. Since the phage has no system for fixing these breaks, phage replication and gene expression is halted. The tracrRNA-crRNA combination can be imitated in a laboratory setting by creating a single-guide RNA (sgRNA) that fulfills the function of both RNA transcripts[6].

Because *Plasmodium* species lack non-homologous end joining[7], the parasite must repair the double-stranded breaks via the homology-directed repair processes. This ensures the integration of plasmids containing coding sequences for the Cas9 protein and sgRNAs into the parasite's genome, assuming they have the appropriate homology. Expression of these components can then be driven by endogenous promoters to target genes within the malaria parasite, specifically those that are stage-specific in order to create a potential vaccine. Whereas, historically, sgRNA were generated using RNA polymerase III and the U6 promoter[8], the Lindner Lab has shown that it is possible to produce functional sgRNAs in *Plasmodium* by cutting the region out of the transcript using ribozymes[9]. This allows for the production of sgRNAs using RNA polymerase II, instead of only with RNA polymerase III, which increases

the number of promoters that can be used to drive expression, allows for the simultaneous production of different sgRNAs, and allows for the use of conditional and stage-specific promoters. The production of functional ribozyme-guide-ribozyme (RGR) transcripts has been previously demonstrated in eukaryotic organisms including a genus of trypanosomes[10] and zebrafish[11]. With the possibility of RGR-sgRNA generation, a variety of promoters can be characterized in terms of their ability to drive their production. Thus, in terms of stage-specific promoters, these could produce sgRNAs capable of targeting multiple essential genes only at specific stages of the parasite's life cycle, thereby causing attenuation of the parasite's development. Therefore, the parasite would be capable of infecting a host (e.g a human), but due to the gene deletions, it would be unable to develop past a certain developmental stage.

In addition to stage-specific promoters, constitutive promoters can be used in a similar way to constantly produce transcripts throughout the life cycle of the parasite. Currently the elongation factor 1 alpha (EF1α) constitutive promoter is used to drive most transgenic in *Plasmodium yoelii*, as well as RGR expression. However, because of its nature as a strong, constitutive promoter, high levels of transcription are present at all times. Additionally, the system being used to produce the Cas9 protein and RGRs consists of a single plasmid containing multiple promoters with each responsible for driving production of the Cas9 protein or the RGRs. These distinct promoters are necessary because the plasmids tend to go through recombination as replication of the plasmid occurs in bacteria. Therefore, if an additional constitutive promoter of similar length and expression levels could be defined, it could greatly decrease the difficulty of future CRISPR-related and other experiments. Therefore, if another constitutive promoter can be adequately characterized it could serve as one of the distinct promoters within the plasmid.

Six promoters, that were previously defined to be stage-specific, were chosen to undergo temporal characterization through the use of immunofluorescence assays[12,13,14,15]. The promoters tested include *CLAG-A*, *DD*, *LAP4*, *TRAP*, *UIS4* and *LISP2*. CLAG-A is a cytoadherence protein involved in binding infected erythrocytic cells to endothelial cells. It has been shown to be specific to the blood stages of the malarial infection namely the ring, trophozoite and schizont developmental stages[12] (figure 2). DD and LAP4 are, likewise, present in blood-stage parasites however, their expression is thought to be exclusive to male and female gametocytes, respectively[13,14]. TRAP is a protein essential for sporozoite motility and is thought to be specific to the mid-to-late midgut stages and the very early salivary gland stage (mosquito phase) of the parasite lifecycle[15]. UIS4 is described as being highly upregulated in the late salivary gland mosquito stage[15] and is known to encode for a parasitophorous vacuole membrane protein. Lastly, LISP2, as indicated by its name, is thought to be a liver-specific protein[14] active in the mid-liver stage that aids in merozoite formation within the host.

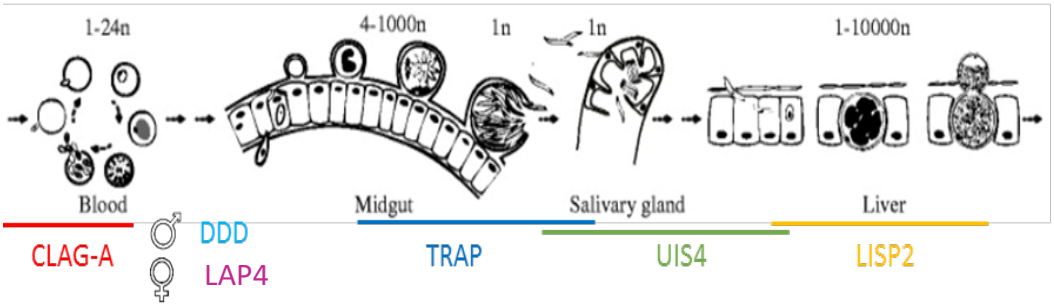

Figure 2. Parasite Life Cycle and Alleged Corresponding Stage-Specific Genes

Figure 2. Parasite Life Cycle and Alleged Corresponding Stage-Specific Genes

In addition to the stage-specific promoters described above, defining additional constitutive promoters would be valuable tools as well. There are a number of housekeeping genes that are known to be expressed to a great degree in many organisms and therefore, we looked to these as a starting point for potential constitutive promoter candidates. Among these

well-expressed genes is HSP70-2/BiP. A known constitutively expressed promoter, HSP70-2/BiP, was tested to determine the relationship between level of expression and different lengths of the promoter. The family of chaperonins known as HSP70s are a well-characterized group of ATPases found in all organisms that facilitate the proper folding of nascent proteins, previously misfolded proteins and the translocation of organellar and secretory proteins[17]. The HSP70-2 gene in particular, is known to be stress inducible and is largely localized to the endoplasmic reticulum. In regards to its expression levels, at least within humans, variance has been shown among different cell types, but it has also been noted that this isoform is the most abundantly produced. This fact particularly speaks to the impetus for selecting this gene's promoter for characterization.

Therefore, the goals of this project were two-fold. First, the identification and characterization of promoters with specific or enriched expression in only one portion of the *Plasmodium* life cycle was undertaken. Second, minimal and maximal variants of the HSP70-2/BiP promoter were defined for potential use as a constitutive promoter. First, with the stage-specific-promoter assays, the individual promoters will be characterized at all stages of the parasite's life cycle through IFAs. This will help verify whether or not these genes are truly stage-specific and thus, if they are suitable for use as a means to produce temporally-regulated sgRNAs for use with Cas9, or other important transgenes. Second, the studies with the BiP promoter could potentially lead to the discovery of another effective, constitutive promoter to drive transgenes such as Cas9 or an RGR RNA. Additionally, by comparing its ability to drive expression to that of EF1α, it could potentially help maximize plasmid-generating efficiency as well as transfection efficacy. Also, if a correlation between expression and length of promoter is seen, this promoter could be used to regulate the amount of sgRNA produced *in vivo*.

Chapter 2

Materials and Methods

Experimental Animals

Six- to eight-week old Swiss Webster female mice, acquired from Envigo, were used for each experiment performed. *Anopheles stephensi* mosquitoes, acquired from the Center for Infectious Disease Research (Seattle, WA) and raised at 24ºC and 70% humidity, were used to experimentally produce *Plasmodium yoelii* parasites. The Pennsylvania State University Institutional Animal Care and Use Committee (IACUC# 42678) approved all experiments performed in this work and each experiment strictly followed the Association for Assessment and Accreditation of Laboratory Animal Care (AAALAC) guidelines.

Generation of Transgenic Parasite Lines Producing GFP Driven by HSP70-2/BiP Promoter Variants

Plasmids intended for use in the production of GFP, which is driven by varying lengths of the HSP70-2/BiP promoter, were generated. Primers (Appendix 2a), identical to the 5' end of the promoter and identical to the appropriate promoter region, were used to amplify the BiP promoter of either 300 or 500 bp in length from pSL1154 (pCR-blunt and 1500 bp PCR product of HSP70-2/BiP promoter from *Plasmodium yoelii* 17XNL genomic DNA) with Phusion polymerase (NEB). The PCR products-of-interest were gel extracted (QIAquick Gel Extraction Kit, Qiagen, Cat# 28706), ethanol precipitated, and ligated into pCR-Blunt (Life Technologies). The plasmids' sizes were checked through restriction digest and the inserted sequences were verified via Sanger Sequencing (Penn State Sequencing Core). Once verified, the promoter sequences were cut from pCR-Blunt using restriction enzymes and ligated into pSL0489, which contains a Green Fluorescence Protein mutant 2 (GFPmut2) cassette for visualization and a

human dihydrofolate reductase (HsDHFR) cassette for drug selection. The sequences ligated into the pSL0489 plasmid served as the promoter for the GFPmut2 cassette. The plasmids were linearized using a restriction enzyme site to cut between the two *p230p* targeting sequences. The linearized plasmid was then precipitated with ethanol, resuspended in water, and transfected into the parasites as described below.

Generation of Transgenic Parasite Lines Producing GFP Driven by Stage-Specific Promoters

Plasmids were produced to express green fluorescence proteins (GFP) by stage-specific promoters. Primers corresponding to the promoter of each selected gene (Appendix 2a), were used to amplify 1500-1800 bp of the desired promoters from purified *Plasmodium yoelii* 17XNL genomic DNA with phusion polymerase (NEB). The desired PCR products were gel extracted (QIAquick Gel Extraction Kit, Qiagen, Cat# 28706), ethanol precipitated, and ligated into an intermediate vector (pCR-Blunt, Life Technologies) to verify the sequences. The size of the plasmid was verified via restriction digest and the sequence was confirmed using Sanger sequencing (Penn State Sequencing Core). Restriction enzymes were used to cut the desired promoter sequence out of the intermediate vector into a pDEF final vector (pSL0489) that has a Green Fluorescence Protein mutant 2 (GFPmut2) cassette for detection and a human dihydrofolate reductase (HsDHFR) cassette for drug selection once in the parasite. The desired promoter sequences were inserted to act as promoters for GFP expression. The plasmid was linearized with a unique restriction enzyme between the targeting sequences for recombination into the *p230p* genomic locus and was transfected as described below.[18]

Synchronization of Schizonts and Accudenz Purification for Transfection

Infected mice were exsanguinated through cardiac puncture. The blood was placed in 5mL complete RPMI (cRPMI; 20% FBS in RMPI 1640 with gentamicin (50 mg/ml (Invitrogen Cat #15750-060))). The blood was centrifuged at 200 *xg* for 8 mins to separate away the serum.

The blood was then resuspended in a closed T75 flask with 30 mL per mouse cRPMI and was mixed with a gas mixture consisting of 5% CO_2, 10% O_2, and 85% N_2. The parasites were cultured for 12 hours at 37 °C on a gradual incline and slightly shaken by an orbital shaker at 50-60 rpm. Following the 12-hour incubation, thin-blood smears were stained with Giemsa to ensure that the parasites had been synchronized to schizonts. After the verification by Giemsa staining, 10 mL of 17% w/v Accudenz dissolved in 5mM Tris pH 7.5, 3mM KCl and 0.3mM EDTA in 1x PBS without calcium and magnesium was layered beneath the 30 mL layer of the parasite culture in a 50ml conical tube. The mixture was then spun at 200 *xg* for 20 mins with no brake. The brown layer containing the parasites, between the accudenz (bottom) and cRPMI (top) layers, was collected. The solution containing the parasites was centrifuged at 200 *xg* for 10 minutes and the supernatant was removed, leaving greater than 10 µL of cRPMI per transfectant.

Transfection and Growth of Parasites

One mg of linearized plasmid in cytomix (120 mM KCl, 0.15 mM $CaCl_2$, 2mM EDTA, 5mM $MgCl_2$, 8.66 mM K_2HPO_4 pH 7.6, 1.34 mM KH_2PO_4 pH 7.6 and 25mM HEPES pH 7.6 at room temperature), was then added to the purified schizonts in cRPMI and they were electroporated[19] using an Amaxa electroporator on program T-016. The transfected parasites were injected intravenously into mice. The mice were placed on pyrimethamine (0.007% w/v, final concentration, Fisher Scientific, Cat# ICN19418025), administered in the drinking water, one day post transfection and remained on drug for three days. After three days of exposure to pyrimethamine, the drug water was replaced with normal water; allowing the parasites to reach a parasitemia of 1%. Infected blood (100 uL) was used to infect a naïve mouse by intraperitoneal injection, and the drug cycling was performed as before. Once 1% parasitemia was reached, the

mouse was exsanguinated, a portion of the infected blood stored in cryovials in liquid nitrogen, with the remainder used to extract genomic DNA for genotyping PCR.

Flow Cytometry

Transgenic parasites containing the 300bp- or 500bp-BIP promoter::GFP plasmid were grown in mice, synchronized to schizonts and accudenz purified as described above. A LSRFortessa (BD), in tube mode, was used to measure the samples' fluorescence and the data was analyzed via FlowJo.

Blood-Stage Immunofluorescence Assay (IFA)

All centrifugation steps occurred at room temperature at 200 *xg* for a duration of 30 seconds.

The blood of infected mice was collected and pelleted. The cells were washed twice with 1x PBS followed by fixation (6% v/v paraformaldehyde, 0.00625% v/v glutaraldehyde in 1x PBS) for 3 hours at room temperature. The cells were then permeabilized, at room temperature, in permeabilization solution (0.1% Triton-100x v/v in PBS) for 10 minutes. Following permeabilization, the cells were mixed with blocking solution (3% w/v bovine serum albumin (BSA) in 1x PBS) and allowed to sit for 1 hour at room temperature. The primary antibodies (rabbit anti-PyACP (1:1000, Pocono Rabbit Farm & Laboratory, Custom polyclonal antibody), rabbit anti-PyCITH (1:1000, Pocono Rabbit Farm & Laboratory, Custom polyclonal antibody), mouse anti-αTub (1:1000, Sigma Aldrich Catalog #T5168), mouse anti-GFP (1:1000, DSHB, Clone 4C9), rabbit anti-GFP (1:1000, Invitrogen, A11122) were diluted in blocking solution, added to the cells and allowed to bind for an hour. After the hour had passed, the cells were

washed twice with 1x PBS and the secondary antibodies (Alexa Fluor-conjugated (AF488, AF594) specific to rabbit or mouse IgG (Invitrogen, Cat# A11001, A11005, A11008, A11012), diluted in blocking solution, were added to the cells. They were allowed to incubate in darkness for an hour. The cells were washed once with 1x PBS and then, DAPI (4′,6-diamidino-2-phenylindole), used to stain the DNA of the parasites, was added, 1μg/mL in 1x PBS, for 5 minutes at room temperature. The cells were washed twice with 1x PBS and mixed 1:1 with VectaShield Hard Set (Vector Laboratories) and applied to a slide and covered with a coverglass slip.

Sporozoite IFA

Sporozoites collected from the midguts or salivary glands of mosquitoes were fixed in ~100 uL of 10% v/v formalin and allowed to incubate for 10-15 minutes at room temperature. They were then centrifuged at top speed in the microcentrifuge for 3 minutes and aspirated. The sporozoites were resuspended in an adequate amount of 1x PBS and their number/uL was determined via a hemacytometer. Twenty-five thousand sporozoites or greater were loaded in each well on a multi-well slide and the slides were allowed to air dry. Following each step after this point, all wells were aspirated with a pipette. The wells were washed with 1x PBS for 2 mins. The sporozoites were then permeabilized with a solution of 0.1% v/v Triton-X 100 for 10 minutes, followed by a wash with 1x PBS and blocking for 1 hr with a solution 10% w/v BSA in 1x PBS. The mixture was then exposed to the appropriate primary antibodies (mouse anti-PyCSP, Clone 2F6 (1:1000 Hybridoma Monoclonal antibody), rabbit anti-GFP (1:1000, Invitrogen, A11122)), diluted in block solution, for 30 minutes. After half an hour, the sporozoites were washed three times with block solution, and then exposed to an appropriate dilution of secondary antibodies (Alexa Fluor-conjugated (AF488, AF594) specific to rabbit or

mouse IgG (Invitrogen, Cat# A11005, A11008)) for 30 additional minutes. The parasites were then washed twice with 1x PBS and incubated, in darkness, with 1ug/mL of DAPI in 1x PBS for 5-10 minutes. Finally, they were then washed three more times in 1x PBS. A small drop of VectaShield Hard Set (Vector Laboratories) was applied to each well containing sporozoites and allowed to dry.

Liver-Stage IFA

Mice livers, infected with *Plasmodium yoelii*, were sliced with a microtome (DSK MicroSlicer Zero1). Two to three liver slices were washed with 1x PBS and placed in a solution of 3% v/v hydrogen peroxide and 0.25% v/v Triton-X 100 in 1x PBS on an orbital shaker for 30 minutes. They were washed again for 10 minutes with 1x PBS and blocked with 5% w/v dried milk in 1x PBS for 1 hour on an orbital shaker. The slices were washed for 10 minutes with 5% w/v dried milk in 1x PBS and exposed to diluted primary antibodies (mouse anti-PyCSP, Clone 2F6 (1:1000 Hybridoma Monoclonal antibody), rabbit anti-PyACP, AmmSO4 Purified (1:1000, Pocono Rabbit Farm & Laboratory, Custom polyclonal antibody), mouse anti-GFP (1:1000, DSHB, Clone 4C9), rabbit anti-GFP (1:1000, Invitrogen, A11122)) for 1 hour. The slices were then washed with 5% w/v dried milk for 10 minutes and exposed to diluted secondary antibodies (Alexa Fluor-conjugated (AF488, AF594) specific to rabbit or mouse IgG (Invitrogen, Cat# A11001, A11005, A11008, A11012), for 2 hours, in darkness, at room temperature while shaking. They were then exposed to DAPI (1 µg/mL) diluted in 1x PBS for 5-10 minutes, in darkness, at room temperature while shaking. They were then washed twice for 10 minutes, exposed to 0.06% w/v potassium permanganate for 20 seconds and washed a final time. The treated liver slices were then placed on a poly-lysine coated microscope slide and VectaShield (Vector Laboratories) was applied and allowed to dry.

Fluorescence Microscopy

A Zeiss Axioscope A1 with 8-bit AxioCam ICc1 camera, using a 63x air or 100x oil objective, was used to perform all live fluorescence and IFA imaging. Live fluorescence was performed to monitor GFP expression in transgenic blood-stage parasites containing the GFP-expression plasmid driven by the 300 and 500 bp BiP promoter as well as transgenic day 7 oocysts. Fluorescence microscopy was used to monitor the other parasite life cycle stages after the appropriate IFA was performed. Zen imaging software was used to process the images.

Mosquito Feeds

Infected blood containing the transgenic parasites-of-interest was injected intraperitoneally into naïve mice to initiate an infection. The number of exflagellation centers within confluent fields of erythrocytes (centers of movement (COMs)) were checked using a 40x lens each day to determine peak transmissibility from mouse to mosquito. When COMs were determined to be at their peak (>1 COM/field), the mice were fed to mosquitoes. This consists of an intraperitoneal (IP) injection of a 100mg/kg ketamine, 10mg/kg xylazine mixture in 1x PBS without calcium and magnesium. The two anesthetized mice per transgenic line were then fed to starved mosquitoes for 15 minutes with rotation occurring every five minutes to allow for even feeding. The midguts of the mosquitoes were dissected seven days after the feed to determine oocyst numbers and the proportion of infected mosquitoes. Three days later (day 10), more mosquito midguts were dissected, ground and the oocysts sporozoites within were counted using a Hausser Bright Line-Phase hemocytometer (Fisher Scientific, Cat# 02-671-6) and stained for IFA. Fourteen days post-feed the salivary glands of the mosquitoes were dissected, ground and the sporozoites were counted using the hemocytometer, and stained for IFA.

Chapter 3

Results

Expression of GFP Using BIP/HSP70-2 Promoter Variants

An additional well-defined constitutive promoter is of interest to our work with CRISPR because of its utility in diversifying the promoter types used to drive expression of Cas9 and ribozyme-guide RNA-ribozyme (RGR) transcripts. These two components are crucial to producing the double-strand breaks associated with the CRISPR gene-modification system. Because only one drug selectable marker is available for use in *P. yoelii*, the coding sequence for both Cas9 and the RGR must be contained within a single plasmid and driven by defined promoters. This plasmid is transfected into the parasites where expression can become active. If the same promoter sequences are used to drive production of both Cas9 and RGR, recombination between these regions on the plasmid can occur within the bacteria thus removing critical portions of the plasmid.

Currently, the *in vivo* production of RGR transcripts is being driven by the EF1α promoter, which is a strong, constitutive promoter that is present in all eukaryotic cell types. This allows for the large-scale, uninterrupted production of RGR transcripts within all stages of the parasite's life cycle. In terms of constitutive production, the EF1α promoter performs well, however the necessity to diversify the variety of constitutive promoters that can drive RGR or Cas9 production to prevent recombination in bacteria has motivated the study and characterization of another constitutive promoter. The new constitutive promoter that was chosen for this purpose was the BiP/HSP70-2 promoter. Like the EF1α promoter, the BiP promoter is active in every cell type making it a prime candidate to drive RGR or Cas9 production. Two truncation variants of the BiP promoter were tested for their activity using a GFP-production

assay. Furthermore, the promoter's relative strength in individual cells was quantitatively compared to that of EF1α via flow cytometry.

Plasmid Generation of Constitutive Promoter Driving GFP

Either a 300 bp or a 500 bp variant of the BiP promoter was inserted into a plasmid (figure 3) upstream of the GFP coding sequence. The plasmids were named pSL1190 and pSL1196, respectively. The plasmid contained homologous regions similar to the *p230p* genetic locus of the parasite, which allowed for recombination following transfection into the parasites. The *p230p* locus was targeted for this work because it is known to be dispensable in every stage of the life cycle[20]. Therefore, no adverse effects will result from recombining into this locus. The transfected parasites were used to infect mice and the parasitemia was allowed to reach ~1%. Furthermore, the genomic DNA (gDNA) was then extracted from the transgenic parasites in order for a genotyping polymerase chain reaction (gPCR) to be performed (figure 4,5). Six distinct primers were designed for gPCR (appendix 2a.), two that are complementary to regions outside of the targeting sequences, two that are complementary to the wild-type *p230p* locus, and two that are complementary to the transgenic gene locus. These were designed such that they can definitively demonstrate that recombination has occurred at the 5' and 3' end of the *p230p* locus. Four reactions each using a different pair of primers were arranged: the first was performed with a primer that binds to the outside of the 5' end of the locus and one that binds within the 5' end of the *p230p* locus (5' WT), the second was performed with a primer that binds to the outside of the 3' end of the locus and one that binds within the 3' end of the wild-type locus (3' WT). The next two used the same 5' and 3' outside primers described in the 5'and 3' WT reactions, but the interior primers used were complementary to the 5' and 3' transgenic locus and are therefore, labeled 5' transgenic (5' TG) and 3' transgenic (3' TG), respectively. In addition to using the

transfected parasite gDNA as a template with the four sets of primers described previously (lanes labelled transfer 1 and/or 2), four additional series of reactions were performed using different DNA templates. These included wild-type parasite gDNA which provides a standard by which to compare the transgenic DNA reaction with the 5' and 3' WT primer sets (Py17XNL (WT)), no template as a negative control (no template control), and pSL1190 or pSL1196 to show that these primers do not generate the correct PCR product if they bind to free plasmid in the reaction mixture (pSL1190/pSL1196). The fourth reaction was also completed using either pSL1190 or pSL1196, but using both primers that bind the interior of the transgenic locus as a positive control to demonstrate that these primers are complementary to those interior regions of the gene (pSL1190/pSL1196 + ctrl).

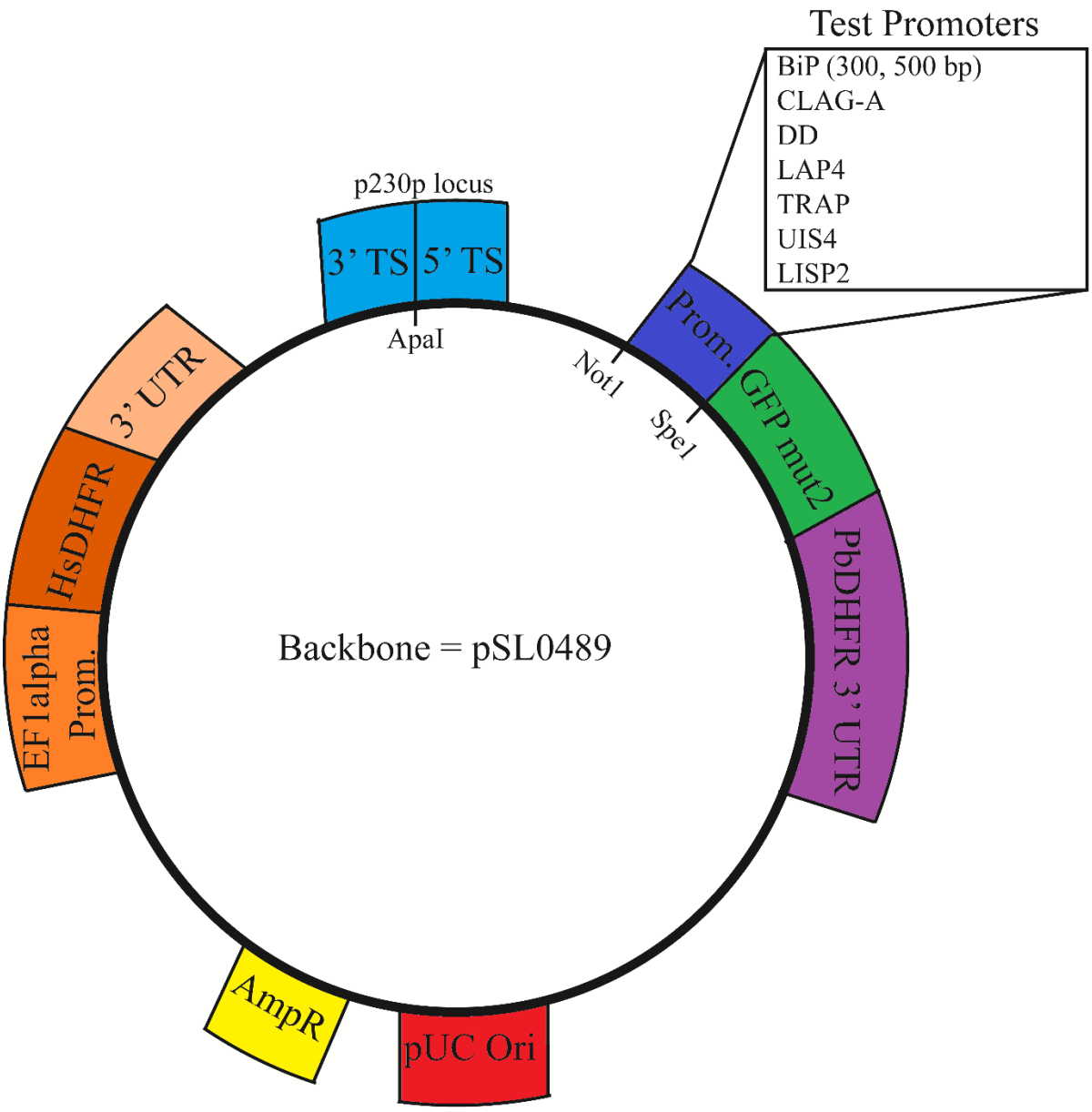

Figure 3. General Vector Map of Plasmids Used for Constitutive and Stage-Specific Promoter Experiments. Each of the plasmids consisted of a pSL0489 backbone with a pUC origin of replication (pUC Ori) and ampicillin resistance gene (AmpR) for selective bacterial amplification within *E. coli*. The plasmid also contained a human dihydrofolate reductase gene (HsDHFR) driven by the EF1α promoter which allows for the selection of purely transgenic parasites in mice. Two targeting sequences, which are separated by an ApaI restriction site that allows for linearization and that are homologous with a 3' or 5' region of the *p230p* genomic locus (3' TS and 5' TS), were included to facilitate integration into the parasite's genome. The coding sequence of GFPmut2 and the 3' UTR of *P. berghei* dihydrofolate reductase (PbDHFR), which has no regulatory effects within *P. yoelii*, driven by the promoter-of-interest (BiP (300 or 500 bp), CLAG-A, DD, LAP4, TRAP, UIS4, and LISP2) were included in the plasmid design.

Figure 3. General Vector Map of Plasmids Used for Constitutive and Stage-Specific Promoter Experiments.

Four distinct bands, one in each lane, were expected in the 5'WT, 3'WT, 5'TG, and 3'TG lanes corresponding to the gDNA collected from the parasites with pSL1190 integrated into the genome (figure 4). In the 5'WT lane a band of 1252 bp was expected, while in 3'WT, 5'TG, and 3'TG bands of 1312 bp, 1537 bp, and 1671 bp, respectively, were expected. Each of these bands were seen in the appropriate lanes indicating that the recombination of pSL1190 into the parasite genome did occur. However, it should be mentioned that despite the gPCR indicating the presence of transgenic parasites, these were in the minority as can be seen from comparing the brightness of the bands corresponding to wild-type and transgenic gDNA. The wild-type parasites only displayed bands in the lanes containing to the wild-type primers. No bands were seen in the no-template-control lanes. A smear of DNA was produced in each of the lanes that contained the products of the PCR using pSL1190 as a template. However, the same distinct band is seen in each of the lanes, but its size does not correspond to the bands expected in the transgenic parasite line. A band of 3037 bp was seen in the plasmid-positive-control lane. Likewise, for the 500 bp variant four distinct bands were expected. The bands expected were of length 1252 bp, 1312 bp, 1730 bp, and 1671 bp for 5'WT, 3'WT, 5'TG and 3'TG, respectively (figure 5). Each of these bands was seen in their appropriate lanes. Therefore, these parasites transfected with pSL1196 can be conclusively called transgenic. It should be noted also that this construct, in comparison to pSL1190, showed far better transfection efficiency as the amount of transgenic gDNA is qualitatively greater than the wild-type. In the associated with wild-type parasite gDNA, the only bands seen were those in the 5'WT and 3'WT lanes. The no-template-control lanes yielded no significant bands. The PCR completed using pSL1196 as a template produced a smear in the lanes, however three distinct bands were seen in each lane as well. But as before, none of these bands is the same size as those expected in the transgenic parasite line.

The pSL1196 plasmid-positive-control lane contained a unique band of 3041 bp. At this point, live fluorescence images were taken to verify the production of GFP within the cytosol of the parasites (figure 6). Green fluorescence was present when the infected cell was visualized while red fluorescence was not, indicating that the fluorescence is due to the presence of the transgenic parasite producing GFP and not autofluorescence. In contrast, wild-type parasites were lacking both green and red fluorescence as expected, because the parasites did not contain an expressible GFP gene. Both promoter variants showed production of GFP via microscopy (figure 6).

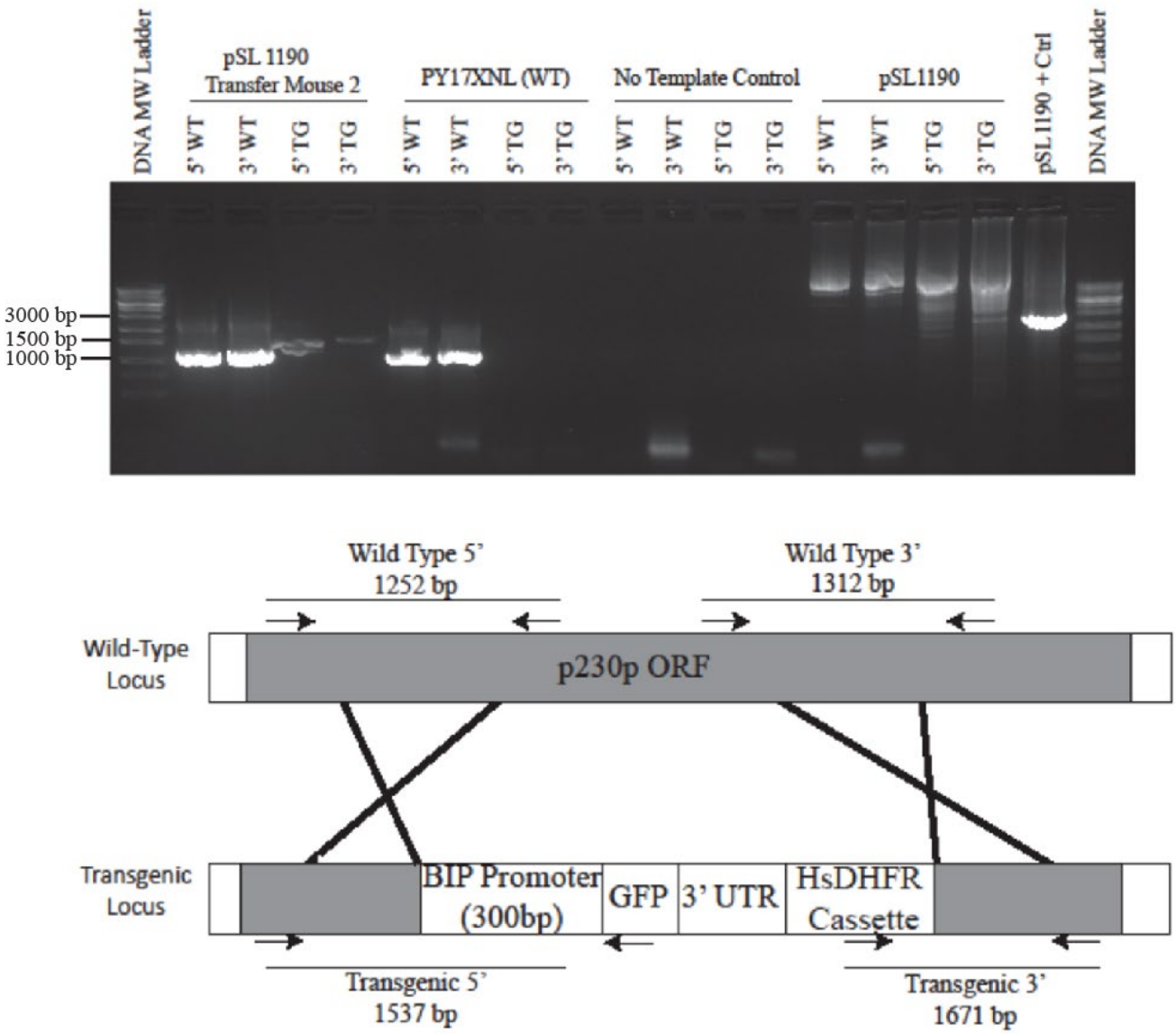

Figure 4. 300 bp BiP Genotyping Polymerase Chain Reaction of Transgenic Parasites. Blood was collected from infected mice and the genomic DNA from the parasites was isolated. A genotyping PCR of the genomic parasite DNA was performed through addition of primers complementary to distinct regions flanking the recombinant target sequences to show proper integration of pSL1190 into the parasite's genome. These clones were compared to a Py17XNL wild-type control, a no template control, and a pSL1190 plasmid positive control.

Figure 4. 300 bp BiP Genotyping Polymerase Chain Reaction of Transgenic Parasites.

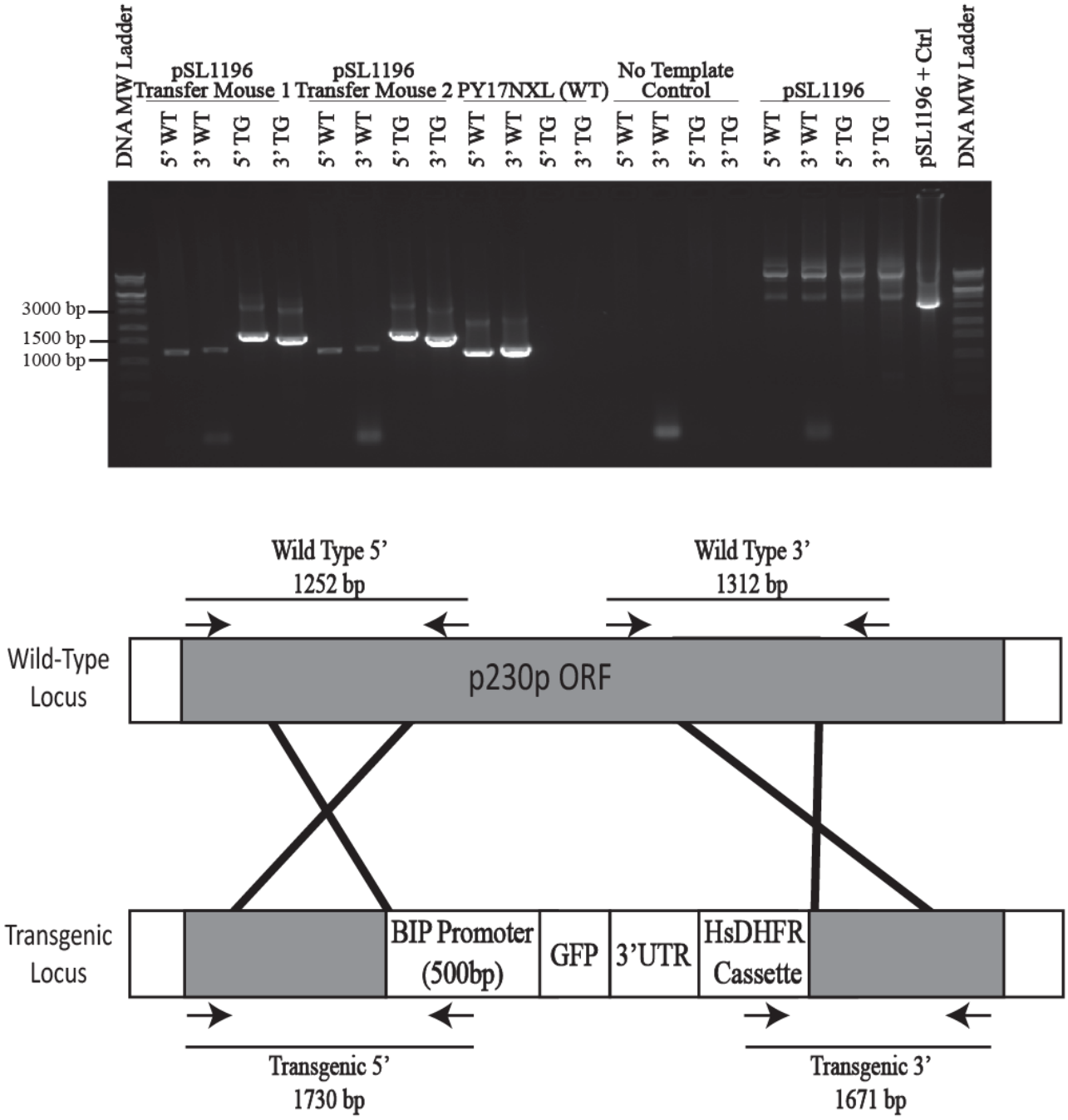

Figure 5. 500 bp BiP of Genotyping Polymerase Chain Reaction of Transgenic Parasites. Blood was collected from infected mice and the genomic DNA from the parasites was isolated. A genotyping PCR of the genomic parasite DNA was performed through addition of primers complementary to distinct regions flanking the recombinant target sequences to show proper integration of pSL1196 into the parasite's genome. These clones were compared to a Py17XNL wild-type control, a no template control, and a pSL1196 plasmid positive control.

Figure 5. 500 bp BiP Genotyping Polymerase Chain Reaction of Transgenic Parasites.

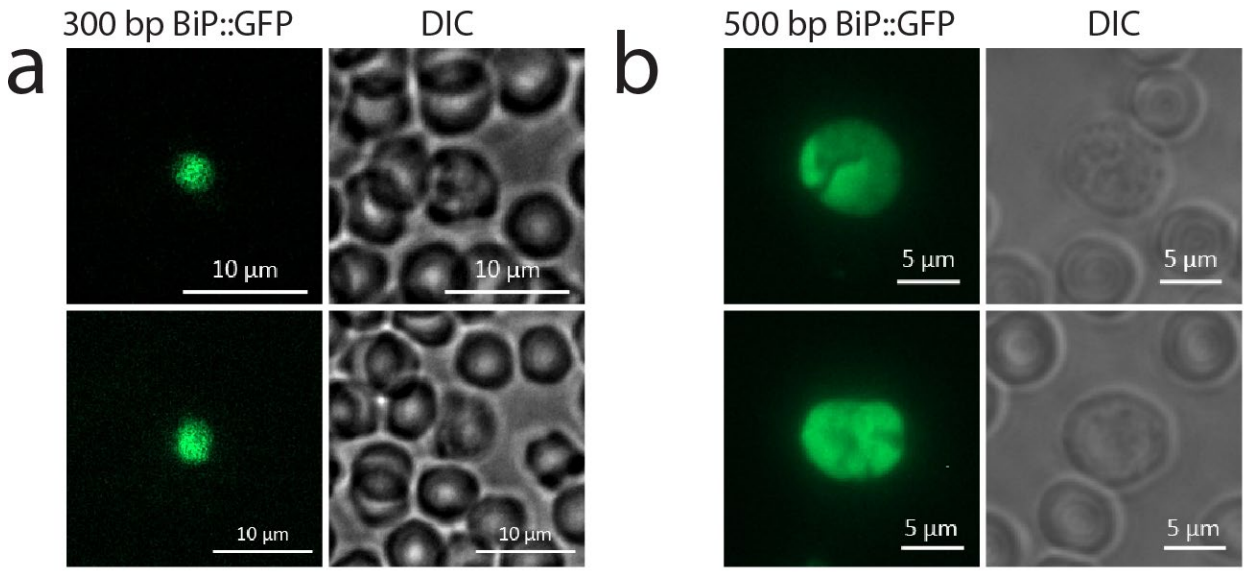

Figure 6. **Live Fluorescence Microscopy of Transgenic Parasites.** a) Parasites were transfected with plasmid containing 300bp variant of HSP70-2/BiP promoter driving GFP followed by integration of plasmid into the *p230p* locus of the parasite genome. b) Parasites were transfected with plasmid containing 500bp variant of HSP70-2/BiP promoter driving GFP followed by integration of plasmid into the *p230p* locus of the parasite genome. Each line of parasites was used to infect mice, extracted, and imaged (figure 6a using 63x air lens and figure 6b with 100x oil lens) to measure GFP expression via fluorescence microscopy.

Figure 6. Live Fluorescence Microscopy of Transgenic Parasites

Quantification of GFP Expression via Flow Cytometry

Once GFP expression was verified via microscopy, mice were again infected with the transgenic parasites containing the 300 and 500 bp HSP70-2/BiP promoter, as well as wild-type parasites (negative control) and transgenic parasites containing a plasmid with EF1α promoter driving GFP (pSL0489 positive control), and allowed to reach a parasitemia of ~1%. The blood was collected and the parasites were synchronized to schizonts. Preceding insertion into the flow cytometer, the cells were treated with DAPI. DAPI is a fluorescent nucleic acid stain that, in this case, allowed infected red blood cells to be distinguished from uninfected. This is because red blood cells naturally lack a nucleus. Two flow cytometry replicates consisting of 100,000 cells each were performed by first selecting for infected cells via their DAPI signal. These cells were then measured for their GFP fluorescence using the appropriate channel.

In both replicates (Figure 7a, b), the wild-type parasites showed little to no GFP expression. The parasites containing pSL0489 showed a range of expression and within this range, three distinct populations (low, medium and high expression) seem to be present. The data from the parasites containing pSL1190 (300 bp BiP variant) showed a small population of cells with very light GFP expression. Comparing the graphs of pSL1190 and the wild-type parasites as a whole, a slight rightward shift of the graph corresponding to the transgenic parasites can be seen indicating a nominal increase in GFP production within a small proportion of the population. This is consistent with the gPCR described earlier, as it indicated that the proportion of wild-type parasites far outnumbered the transgenic. However, in general the amount of GFP fluorescence in pSL1190 populations does not differ greatly from the wild-type parasites. This suggests that during live fluorescence microscopy, autofluorescence in the transgenic parasites

containing pSL1190 may have contributed to the detected signal. Alternatively, the flow cytometer using the chosen settings may not have been sensitive enough to be able to distinguish between the background fluorescence and the GFP expression driven by the 300 bp construct. The transgenic parasites containing pSL1196 (500 bp BiP variant) showed significant levels of brightness similar to the pSL0489-containing parasites. The range of expression for this line of parasites had a similar minimum to the pSL0489 transgenic parasite, but the maximum was slightly less, indicating that 500 bp HSP70-2/BiP promoter has a relative promoter strength similar to EF1α. The parasites showing expression were distributed into three distinct populations corresponding to the low-, medium- and medium-high-expression ranges described in relation to the positive control parasites. Parasites with a high level of expression were lacking in this data set. Compared to the pSL0489 parasites, there were fewer pSL1196-containing parasites that showed appreciable fluorescence. Comparing the two graphs, it can be seen that pSL0489 has a greater number of low-expressing parasites, while pSL1196 has a greater number of medium-fluorescent parasites. In comparing the 300 bp and 500 bp constructs, it can be seen that the promoter strength varies substantially between the two, with the larger variant driving a greater level of transcription. This thereby demonstrates that the 200 bp portion of the promoter missing from the 300 bp variant alters gene expression to a significant degree. The average and median expression values for each of these populations were not included here, because these samples contained both GFP+ transgenic and non-fluorescent wild-type parasites, but to differing degrees.

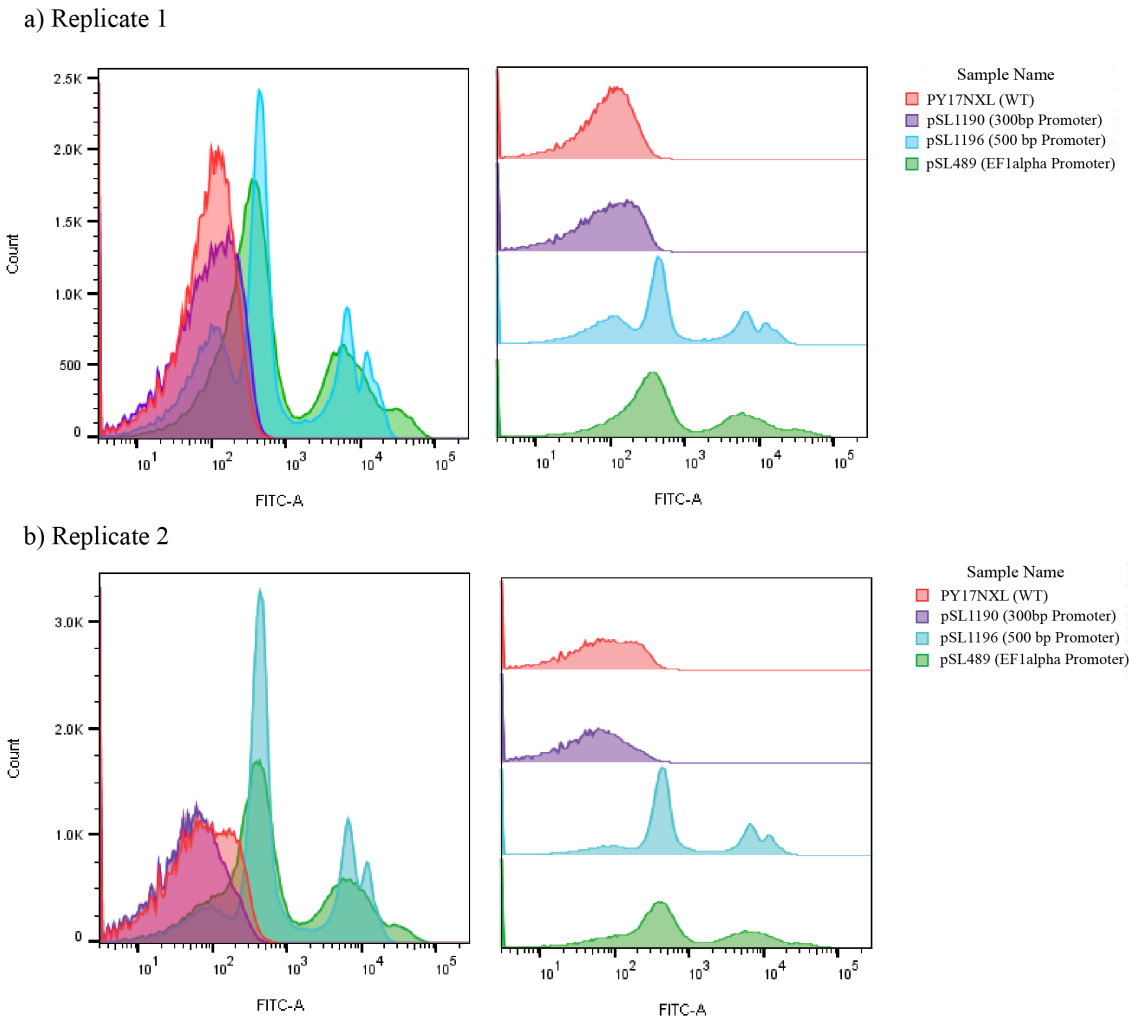

Figure 7. Distribution of parasites in regard to brightness of GFP fluorescence. a) Replicate 1 (a) and 2 (b) overlay the distributions of all red blood cells in terms of the brightness of GFP-fluorescent parasites contained within each sample type (red: WT; blue: pSL489; purple: pSL1190; yellow: pSL1196).

Figure 7. Distribution of parasites in regard to brightness of GFP fluorescence.

Characterization of Stage-Specific Promoters for CRISPR/Cas9 Production

Plasmids containing the six stage-specific promoters-of-interest (CLAG-A, DD, TRAP, LAP4, LISP2 and UIS4) driving GFP expression were generated in a two-step process involving insertion of the PCR amplified promoter into an intermediate vector (pCR-blunt; pBS2254) for sequence validation, followed by insertion of the promoter into the final vector (pDEF-GFP; pSL0489). These plasmids (Table 1) were generated by Laura Bowman, a former lab member,

who was working on characterizing these promoters prior to graduating[18]. pSL0489 has targeting regions that are homologous to the *Plasmodium yoelii p230p* genetic locus, allowing for double homologous recombination to occur after transfection. All of the plasmids with a pSL0489 backbone were shown by gPCR[16] to properly insert into the genome of the parasite.

Table 1. Plasmids of Stage-Specific Promoters Driving GFP Expression

Table 1. Plasmids of Stage-Specific Promoters Driving GFP Expression[18]. This table is adapted from the thesis of a former undergraduate lab member, Laura Bowman, who generated the plasmids listed below. The table lists the plasmids according to their identifiers (pSLXXXX), the stage-specific promoter present, the parent vectors from which they were made, and the antibiotic resistance gene present and used for selection in bacteria. The first six plasmids are the intermediate vectors consisting of the stage-specific promoter and pCR-blunt. The last six plasmids are the final vectors used for transfection into the parasites and capable of recombination.

Plasmid name	Description	Parent Vectors	Antibiotic Resistance
pSL0987	CLAG-Aprom-2254 (antisense)	pBS2254, PCR product	Kan
pSL0983	DDprom-2254 (sense)	pBS2254, PCR product	Kan
pSL0981	LAP4prom- 2254 (sense)	pBS2254, PCR product	Kan
pSL1008	TRAPprom-2254 (sense)	pBS2254, PCR product	Kan
pSL0738	UIS4prom-2254 (sense)	pBS2254, PCR product	Kan
pSL0988	LISP2prom-2254 (sense)	pBS2254, PCR product	Kan
pSL1058	pDEF-CLAG-Aprom-GFP	pSL0489, pSL0987	Amp
pSL1020	pDEF-DDprom-GFP	pSL0489, pSL0983	Amp
pSL1019	pDEF-LAP4prom-GFP	pSL0489, pSL0981	Amp
pSL1082	pDEF-TRAPprom-GFP	pSL0489, pSL1008	Amp
pSL1083	pDEF-UIS4prom-GFP	pSL0489, pSL0738	Amp
pSL1017	pDEF-LISP2prom - GFP	pSL0489, pSL0988	Amp

Live Fluorescence and Indirect Immunofluorescence Assays

The transgenic parasites were allowed to progress through the lifecycle and were assessed by live fluorescence and/or indirect immunofluorescence assays (IFAs). Portions of this work, including the live fluorescence imaging of all day 7 oocysts, and the IFAs of the day 10 and 14 sporozoite and 24- and 48-hr liver-stage parasites of CLAG-A, DD and LAP4, were completed

by Laura Bowman as a part of her thesis project[18]. Expression of GFP, or lack thereof, was visualized by IFA with anti-GFP in each of the asexual-blood stages (ring, trophozoite and schizont) as well as in male and female gametocytes as determined by the staining with an appropriate antibody (asexual-blood-stage parasite: ACP, male gametocytes: α-tubulin, female gametocytes: CITH). Oocysts were not treated with antibodies but were rather monitored for GFP expression via live fluorescence microscopy. Day-10 and 14 sporozoites were exposed to the appropriate antibody (anti-CSP and anti-GFP) and expression was determined via fluorescence microscopy. Similarly, 24-hr and 48-hr liver stages were checked for expression likewise through exposure with the appropriate antibodies (24-hr: ant-CSP, 48-hr: ACP, and anti-GFP). In addition, late in the completion of this work, single-cell transcriptomics for *P. berghei* became available via the Wellcome Sanger Institute's Malaria Cell Atlas prior to publication. This data (Appendix 1a-h) is discussed in relation to the IFA and live fluorescence data collected in this work further in Chapter 4 (Discussion) of this paper.

The first stage-specific promoter that was tested was CLAG-A; it was expected to be present in the asexual parasite stages. As anticipated, expression was seen in rings, trophozoites and schizonts, however it was likewise seen, albeit to a lesser extent, in the sexual stages (figure 8). A previous publication[21] utilized this promoter in a promoter swap experiment such that a protein-of-interest would be selectively expressed in asexual blood-stage parasites but not male or female gametocytes. However, the IFA data presented here indicates that this experimental design would not function as intended, as GFP expression is driven by CLAG-A in both asexual and sexual blood stages. This data is further corroborated by transcriptomic and proteomic experiments, described in Chapter 4, which similarly indicate that CLAG-A is not specific to asexual blood stages. Additionally, previous data demonstrated that the CLAG-A promoter is

active in the mosquito and liver stages of the parasite's lifecycle, with GFP expression seen in 7-day oocysts and at the 48-hour liver stage[18].

Next, the DD promoter was tested. This promoter was expected to be active in male gametocytes. A very high level of expression was seen in male gametocytes, but was also seen, to a low extent, in schizonts (figure 9). No expression was seen in trophozoites. GFP expression in other stages, as determined by mosquito- and 48- hour liver-stage IFAs performed previously, was determined to be absent[18]. An IFA performed at the 24-hour liver stage revealed that there was also no expression of GFP at this life-cycle stage (figure 10).

The GFP expression driven by the LAP4 promoter was tested next. LAP4 is described to be a female gametocyte-specific promoter. Despite this, low levels of expression were seen in each of the asexual-blood stages (figure 11). Expression was seen in female gametocytes, but also to the same degree in male gametocytes. This is a significant discovery because prior studies[19] have used the LAP4 gene as a way of specifically demarcating female gametocytes. However, this IFA data suggests caution should be urged with this strategy, as transcription from this promoter can be as high in male gametocytes as it is in female gametocytes. Previous work also indicated that no expression was seen in oocysts, sporozoites or in the liver stages[18].

The mid-to-late-mosquito-stage promoter, TRAP, was then tested. As expected, no expression was seen in rings, sporozoites or schizonts (figure 12). However, low expression was seen in male gametocytes and the expression in female gametocytes was mixed, that is ~50% of the female gametocytes visualized showed light expression while the other half had no expression. Previous data[18] revealed that GFP expression was not seen in early day-7 oocysts, which is consistent with previous studies showing that it is not active until the later oocyst

stage[15]. GFP expression in day-14 sporozoites revealed that the TRAP promoter was active at this stage, which is consistent with previous data (figure 13).

UIS4 was thought to solely be active in the salivary glands of the mosquito, and thus was defined as a late-mosquito stage promoter. The IFAs performed to test UIS4 promoter activity yielded unanticipated results. Mixed expression was seen in rings, no expression was seen in trophozoites, while low expression was seen in schizonts (figure 14). Similarly, low expression was seen in male and female gametocytes. Additionally, it was demonstrated that there was expression in day-7 oocysts[18]. Day-10 sporozoites did not display any expression (figure 15) while day-14 sporozoites displayed light green fluorescence compared to background indicating that this promoter is active to a small degree in this stage (figure 13). Micrographs of 24-hour liver stage IFAs showed extremely high expression of GFP in this stage of the parasite's life cycle (figure 10) while very light expression was seen in the 48-hour liver stage (figure 16). This could indicate that in the 48-hour liver stage no actual production of GFP is occurring but rather the GFP seen in this stage is the result of carryover from the previous stage due to the relatively long half-life of GFP (e.g. 24 hours).

Finally, the stage-specificity of LISP2 was assayed. The IFAs revealed that, despite being thought to only be active in liver stage parasites, there is some activity, at a low level, in female gametocytes (figure 17). This was the only blood stage that showed expression. Expression was also not seen in day-7 oocysts.

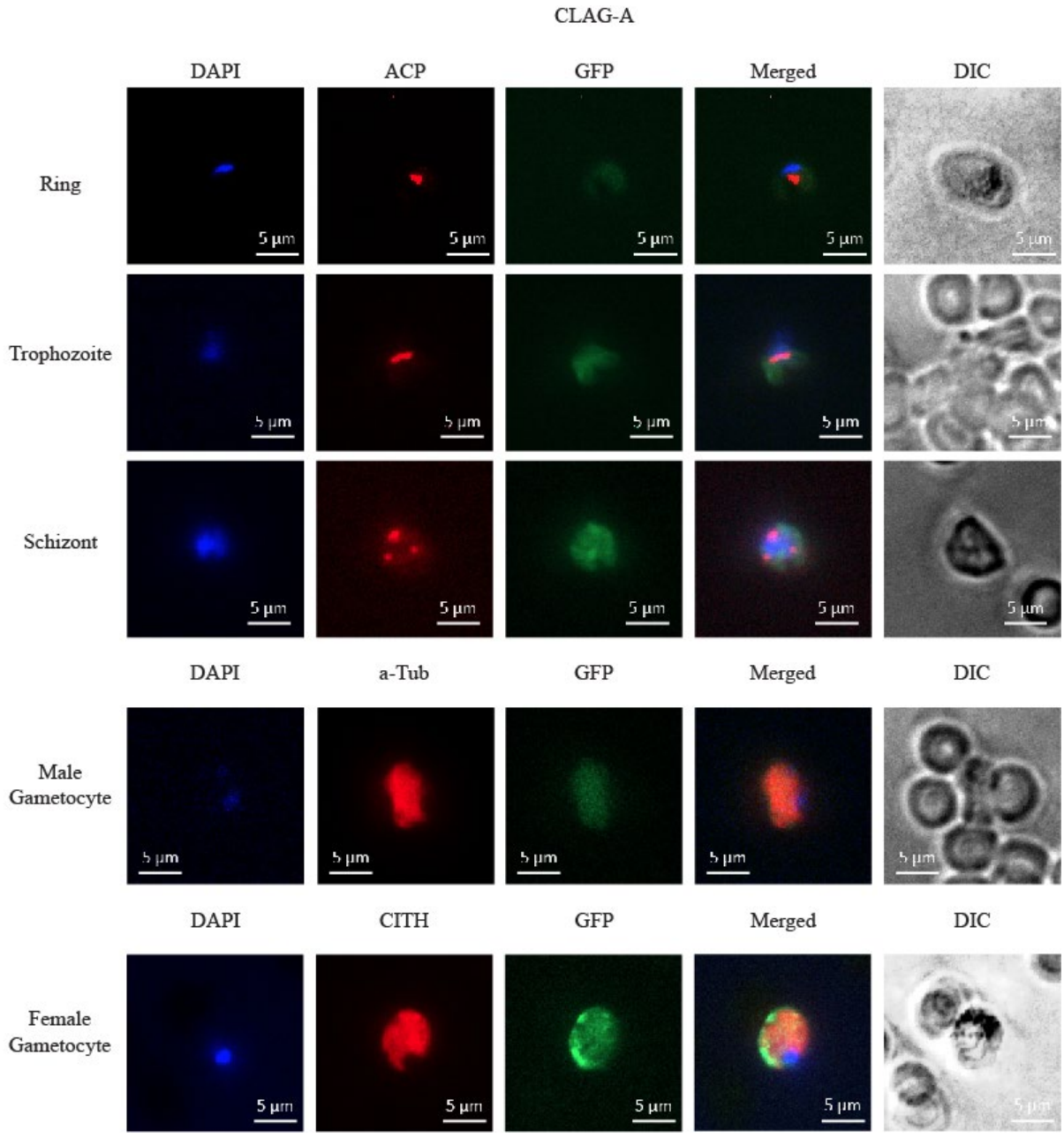

Figure 8. Blood-Stage IFAs Determining CLAG-A Promoter Activity. Rings, trophozoites, schizonts, as well as male and female gametocytes, were extracted from Swiss Webster mice when parasitemia reached 1% and stained with the noted primary and secondary antibodies. The fluorescence was visualized (from left to right) with the following channels: DAPI (blue), ACP (red; asexual-blood stage)/α-Tubulin (red; male gametocyte)/CITH (red; female gametocyte), GFP (green), merged and DIC. Infected cells were determined via the presence of DAPI. Each of the blood stages showed GFP expression driven by CLAG-A.

Figure 8. Blood-Stage IFAs Determining CLAG-A Promoter Activity.

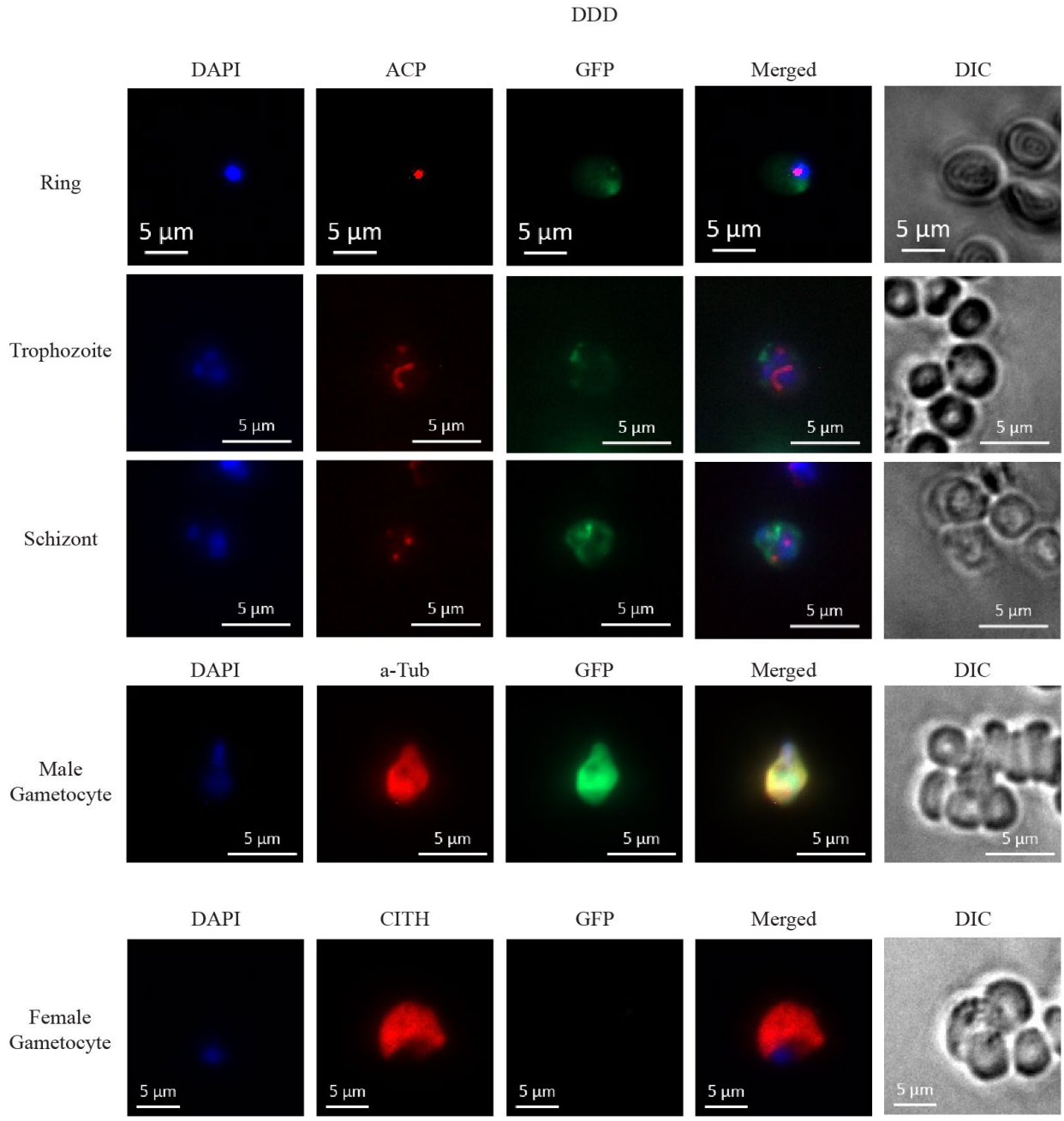

Figure 9. Blood-Stage IFAs Determining DD Promoter Activity. Rings, trophozoites, schizonts, as well as male and female gametocytes, were extracted from Swiss Webster mice when parasitemia reached 1% and stained with the noted primary and secondary antibodies. The fluorescence was visualized (from left to right) with the following channels: DAPI (blue), ACP (red; asexual-blood stage)/α-Tubulin (red; male gametocytes)/CITH (red; female gametocytes), GFP (green), merged and DIC. Infected cells were determined via the presence of DAPI. The asexual-blood stage and male gametocytes showed GFP expression when driven by DD.

Figure 9. Blood-Stage IFAs Determining DD Promoter Activity.

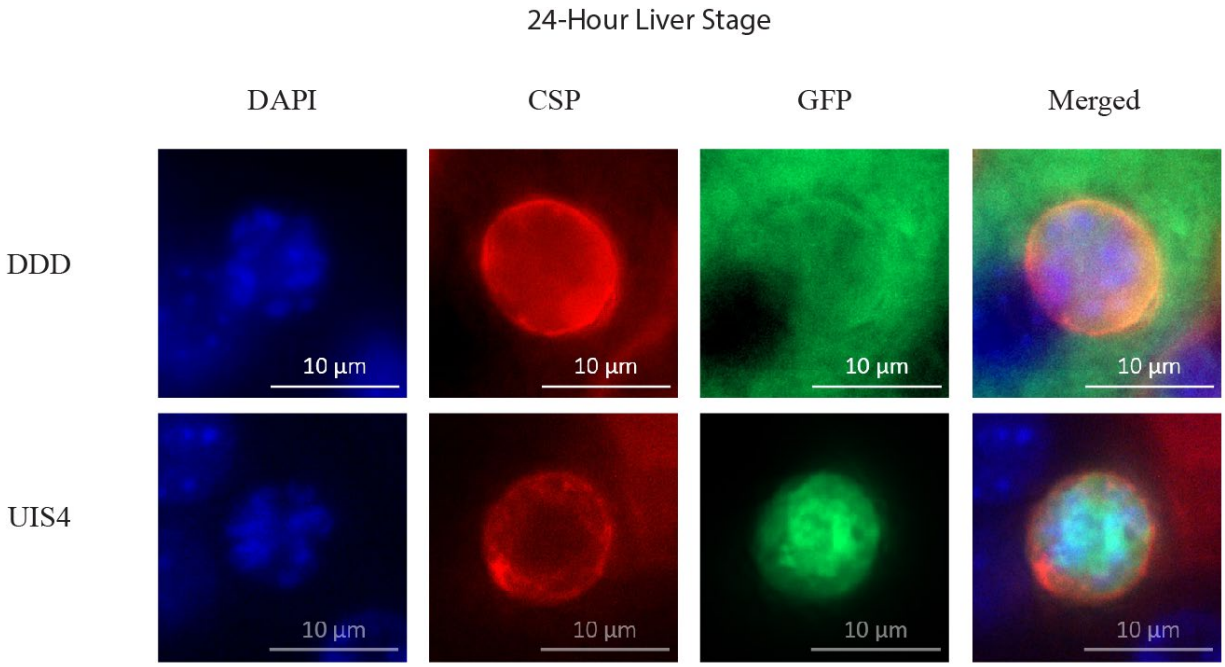

Figure 10. 24-Hour Liver- Stage IFAs Stage-Specific Promoter Activity. Salivary gland sporozoites were injected into the tail vein of Swiss Webster mice and at 24 hours the livers of the mice were removed. The livers were cut into 50-micron thick slices and stained with the noted primary and secondary antibodies. The fluorescence was visualized (from left to right) with the following channels: DAPI (blue), CSP (red), GFP (green) and merged. Infected cells were determined via the presence of ACP.

Figure 10. 24-Hour Liver-Stage IFAs Stage-Specific Promoter Activity

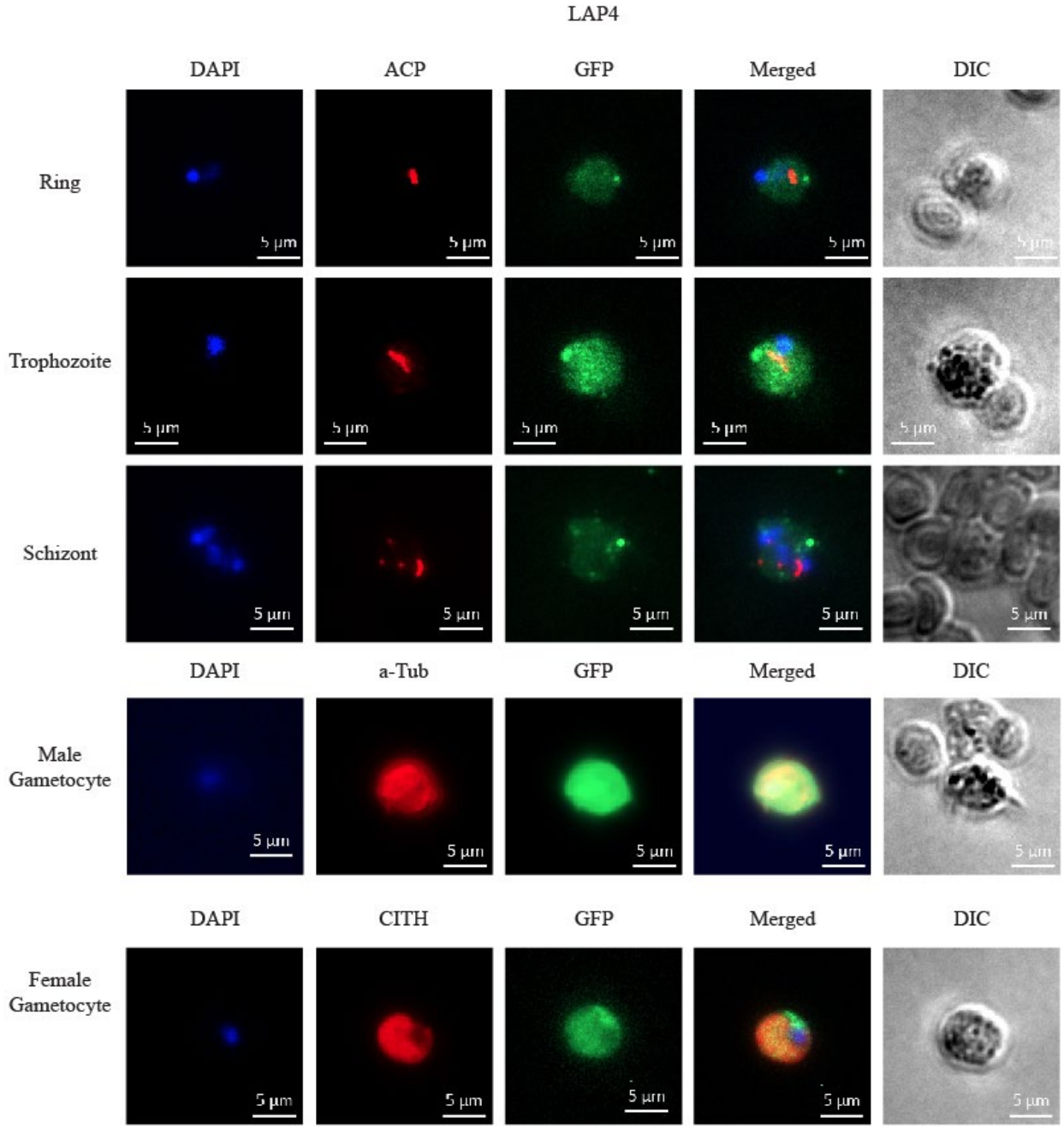

Figure 11. Blood-Stage IFAs Determining LAP4 Promoter Activity. Rings, trophozoites, schizonts, as well as male and female gametocytes, were extracted from Swiss Webster mice when parasitemia reached 1% and stained with the noted primary and secondary antibodies. The fluorescence was visualized (from left to right) with the following channels: DAPI (blue), ACP (red; asexual-blood stage)/α-Tubulin (red; male gametocytes)/CITH (red; female gametocytes), GFP (green), merged and DIC.

Figure 11. Blood-Stage IFAs Determining LAP4 Promoter Activity.

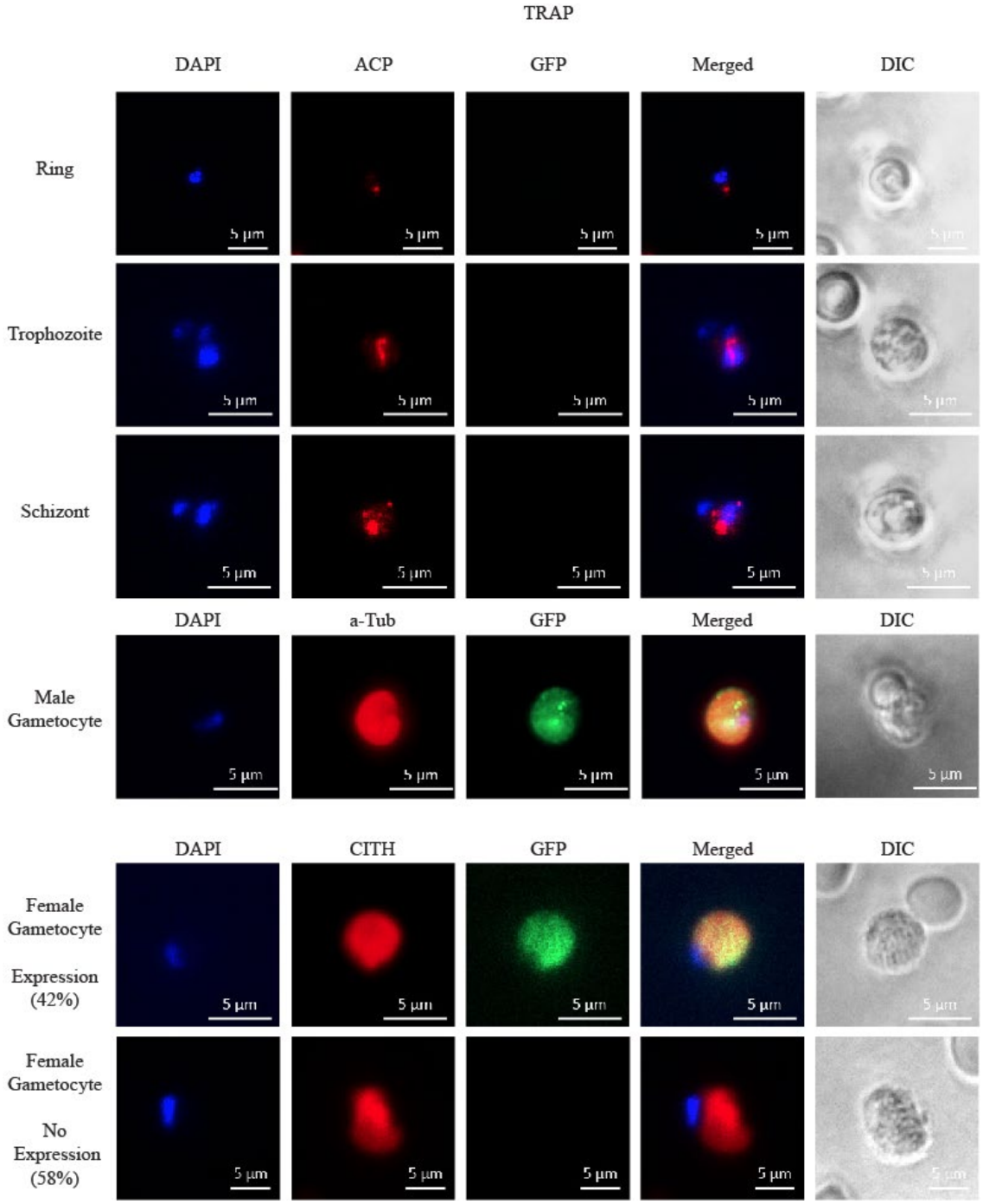

Figure 12. Blood-Stage IFAs Determining TRAP Promoter Activity. Rings, trophozoites, schizonts, as well as male and female gametocytes, were extracted from Swiss Webster mice when parasitemia reached 1% and stained with the noted primary and secondary antibodies. The fluorescence was visualized (from left to right) with the following channels: DAPI (blue), ACP (red; asexual-blood stage)/α-Tubulin (red; male gametocytes)/CITH (red; female gametocytes), GFP (green), merged and DIC. Infected cells were determined via the presence of DAPI. All male and 42% of female gametocytes showed GFP expression when driven by TRAP.

Figure 12. Blood-Stage IFAs Determining TRAP Promoter Activity

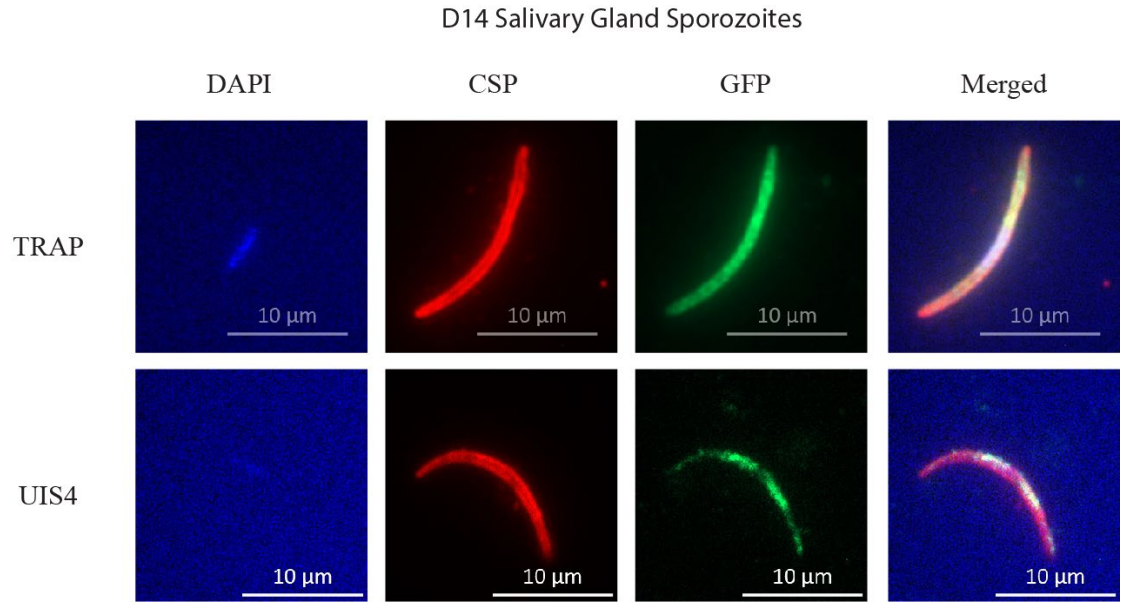

Figure 13. D14 Sporozoite IFAs Stage-Specific Promoter Activity. Mosquito salivary glands were dissected and lysed at 14 days post feed to release sporozoites. The sporozoites were purified away from remaining mosquito debris and exposed to the appropriate primary and secondary antibodies. The fluorescence was visualized (from left to right) with the following channels: DAPI (blue), CSP (red), GFP (green) and merged.

Figure 13. D14 Sporozoite IFAs Stage-Specific Promoter Activity.

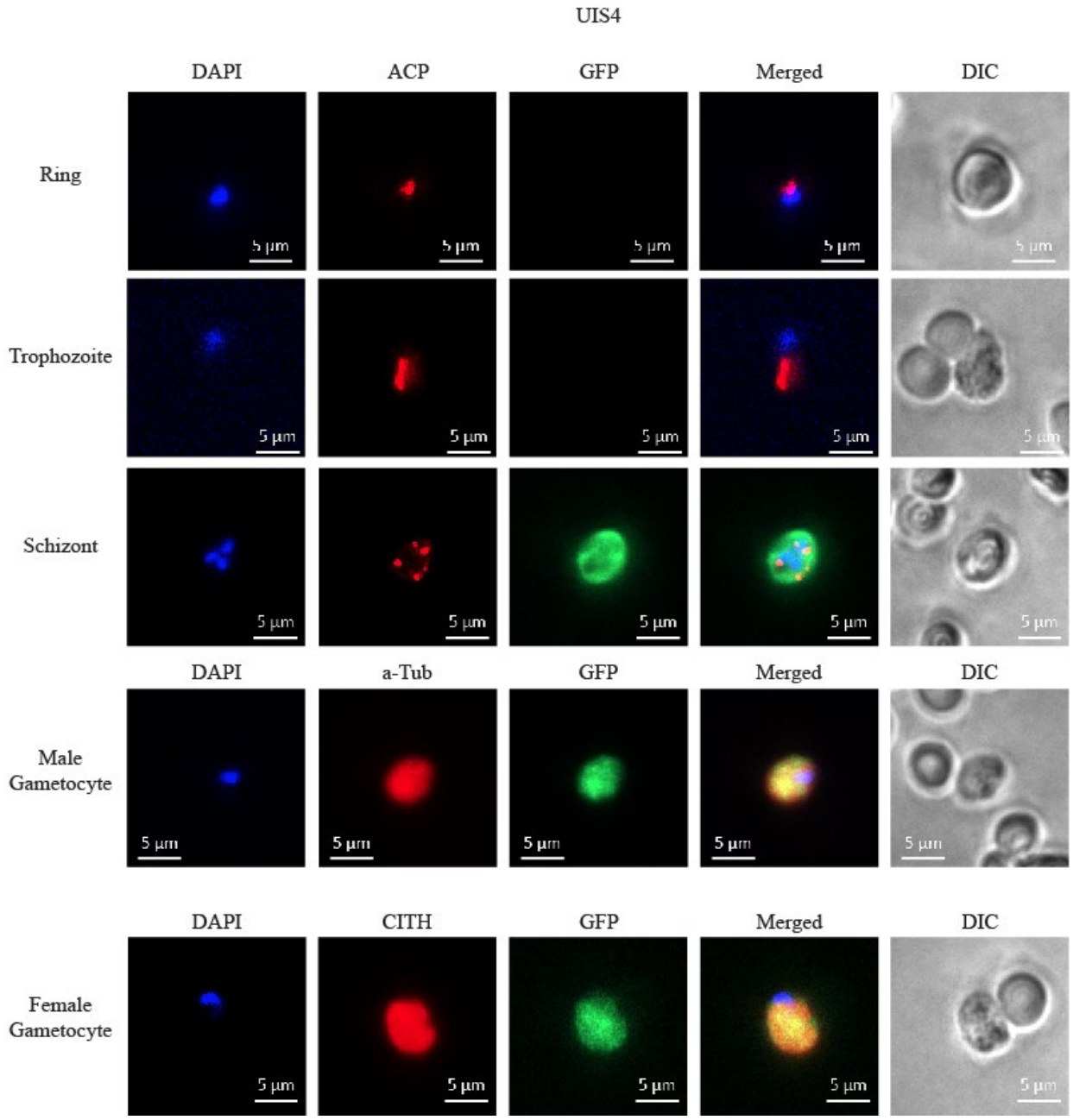

Figure 14. Blood-Stage IFAs Determining UIS4 Promoter Activity. Rings, trophozoites, schizonts, as well as male and female gametocytes were extracted from Swiss Webster mice when parasitemia reached 1% and stained with the noted primary and secondary antibodies. The fluorescence was visualized (from left to right) with the following channels: DAPI (blue), ACP (red; asexual-blood stage)/α-Tubulin (red; male gametocytes)/CITH (red; female gametocytes), GFP (green), merged and DIC. Infected cells were determined via the presence of DAPI. All schizonts, and all female and male gametocytes showed GFP expression when driven by UIS4.

Figure 14. Blood-Stage IFAs Determining UIS4 Promoter Activity.

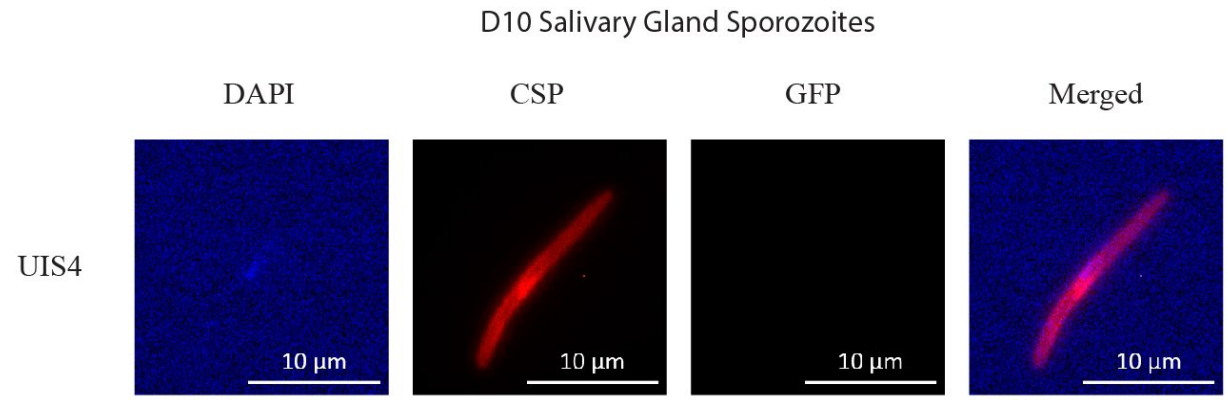

Figure 15. D10 Sporozoite IFAs Stage-Specific Promoter Activity. Mosquito midguts were dissected and lysed at 10 days post feed to release sporozoites. The sporozoites were purified away from remaining mosquito debris and exposed to the appropriate primary and secondary antibodies. The fluorescence was visualized (from left to right) with the following channels: DAPI (blue), CSP (red), GFP (green) and merged.

Figure 15. D10 Sporozoite IFAs Stage-Specific Promoter Activity.

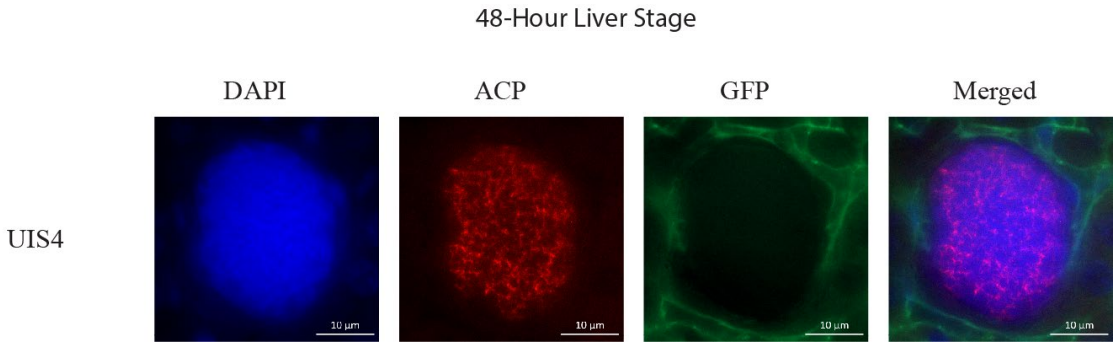

Figure 16. 48-Hour Liver- Stage IFAs Stage-Specific Promoter Activity. Salivary gland sporozoites were injected into Swiss Webster Mice and at 48 hours the livers of the mice were removed. The livers were cut into 50-micron slices and exposed to the appropriate primary and secondary antibodies. The fluorescence was visualized (from left to right) with the following channels: DAPI (blue), ACP (red), GFP (green) and merged. Infected cells were determined via the presence of ACP.

Figure 16. 48-Hour Liver- Stage IFAs Stage-Specific Promoter Activity.

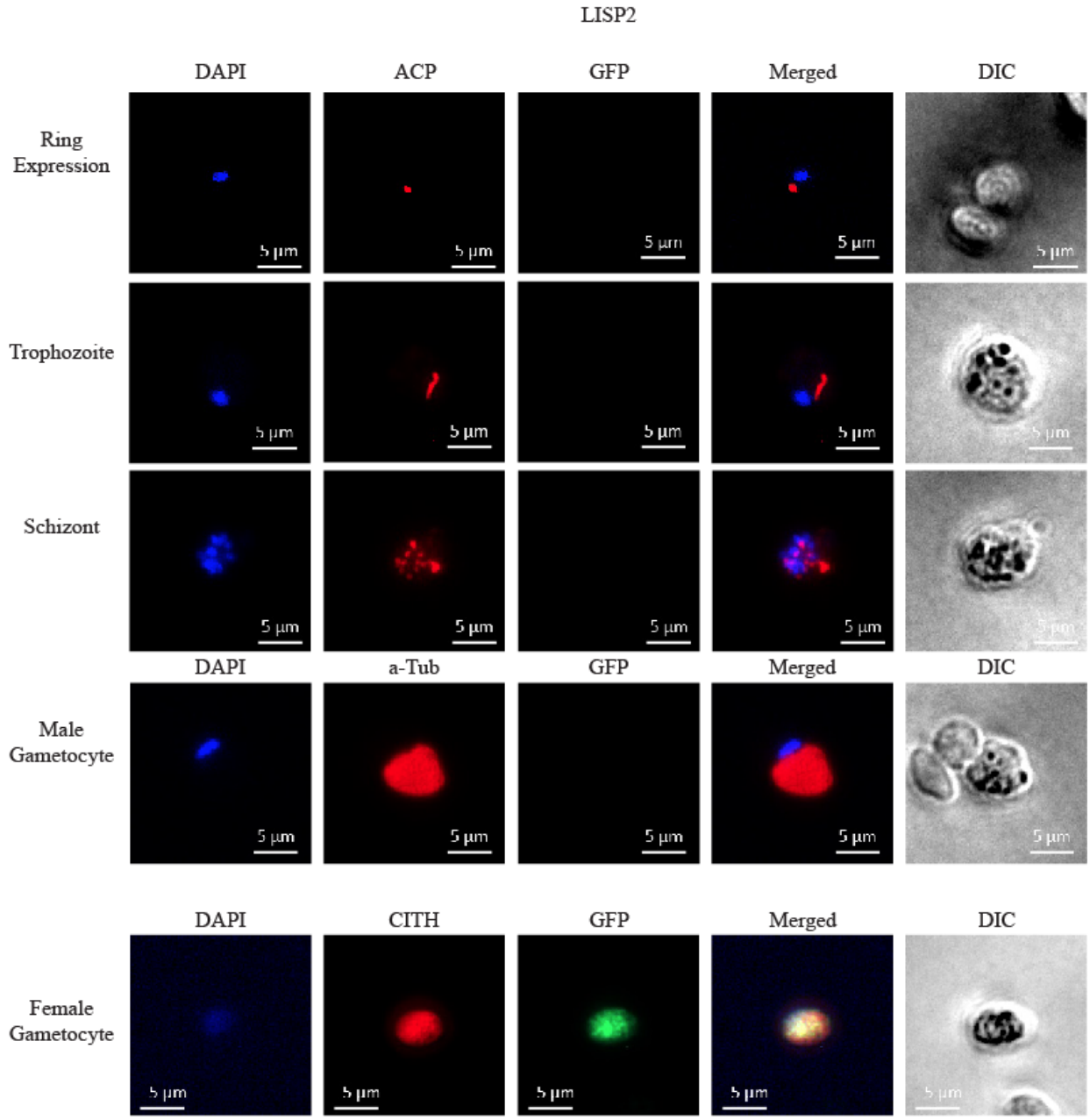

Figure 17. Blood-Stage IFAs Determining LISP2 Promoter Activity. Rings, trophozoites, schizonts, as well as male and female gametocytes, were extracted from Swiss Webster mice when parasitemia reached 1% and stained with the noted primary and secondary antibodies. The fluorescence was visualized (from left to right) with the following channels: DAPI (blue), ACP (red; asexual-blood stage)/α-Tubulin (red; male gametocytes)/CITH (red; female gametocytes), GFP (green), merged and DIC. Infected cells were determined via the presence of DAPI. Female gametocytes showed GFP expression when driven by LISP2.

Figure 17. Blood-Stage IFAs Determining LISP2 Promoter Activity.

Gene ID	Promoter	Blood Stage				
		Ring	Trophozoite	Schizont	Male gametocytes	Female gametocytes
PY17X_1402200	**CLAG-A**	expression	expression	expression	low expression	low expression
PY17X_0418900	**DD**	no expression	no expression	low expression	high expression	no expression
PY17X_1323300	**LAP4**	low expression	low expression	low expression	expression	expression
PY17X_1354800	**TRAP**	no expression	no expression	no expression	low expression	mixed
PY17X_0502200	**UIS4**	no expression	no expression	low expression	low expression	low expression
PY17X_1004400	**LISP2**	no expression	no expression	no expression	no expression	low expression

Gene ID	Promoter	Early Mosquito Stage (Live Fluorescence)	Late Mosquito Stage		Liver Stage	
		Oocyst D7	Sporozoite D10	Sporozoite D14	24H	48H
PY17X_1402200	**CLAG-A**	high expression	no expression	no expression	no expression	high expression
PY17X_0418900	**DD**	no expression	no expression	no expression	no expression	no expression
PY17X_1323300	**LAP4**	no expression	no expression	no expression	no expression	no expression
PY17X_1354800	**TRAP**	no expression		expression		
PY17X_0502200	**UIS4**	expression	no expression	low expression	high expression	low expression
PY17X_1004400	**LISP2**	no expression				

Table 2. Summary of Expression of GFP under Stage-Specific Promoters

Table 2. Summary of Expression of GFP under Stage-Specific Promoters. Summary of GFP expression as it was driven by the listed stage-specific promoter in certain stages of the parasite's lifecycle. If GFP expression was seen then the subjective level of expression in terms of GFP intensity by microscopy was described. Some of this work was performed and compiled by Laura Bowman as part of her honors thesis.

Chapter 4

Discussion

Current production of exogenous proteins (e.g. Cas9, recombinases) and RNAs (e.g. Ribozyme-Guide-Ribozyme transcripts) in *Plasmodium yoelii* rely on expression from a single plasmid, as only one drug selectable marker is available for use. In the case where multiple gene products must be expressed, at least two distinct promoters should be used to prevent unwanted recombination events that can occur when sequences are repeated. The heat-shock family of proteins is known to be constitutively expressed, as they are integral to the proper folding of proteins. Therefore, I investigated the use of the HSP70-2/BiP promoter for the continuous production of GFP. Furthermore, variants of this promoter were tested to determine their relative strengths compared to the well-defined constitutive EF1α promoter.

This study was performed using two plasmids, capable of recombination into the parasite's dispensable *p230p* genetic locus, which contained either a 300 bp or 500 bp variant of the HSP70-2/BiP promoter driving GFP so that expression could be measured qualitatively and quantitatively. GFP expression was visualized using live fluorescence microscopy and the objective brightness of the cells was measured via flow cytometry. The live fluorescence imaging indicated that GFP production was occurring when both promoter lengths were used. Flow cytometry revealed that GFP was in fact being produced at a detectable level and above the background fluorescence of wild-type parasites. However, compared to the parasites using EF1α to drive GFP expression, both HSP70-2 variants showed considerably less expression in maximum brightness across the infected cell population. This suggests that, while neither promoter is capable of producing GFP to the same degree as the EF1α promoter, there could be some use for these promoter variants when very low or moderate expression is desired. In

addition, flow cytometry demonstrated that the 500 bp and 300 bp variants differed in promoter strength as indicated by the different levels of fluorescence produced.

The Malaria Cell Atlas was consulted to verify that the HSP70-2/BiP promoter is truly constitutive. Expression levels of BiP range from very low to almost none in schizonts to very high in a large percentage in oocysts and trophozoites as well as a majority of rings. Additionally, the expression in male gametocytes, female gametocytes, and sporozoites can be described on average as intermediate expression, however there is large disparity between individual cells (appendix 1a). Therefore, while this promoter appears to be active in all of the life-cycle stages, except for the majority of schizonts, variation in expression levels of a protein-of-interest being driven by this promoter, such as Cas9 or RGRs, will depend on the stage in which the experiment is to take place and, to an extent, the individual cells within those stages. Furthermore, the Malaria Cell Atlas was used to compare HSP70-2/BiP expression to that of EF1α. Surprisingly, the Atlas revealed that, despite being a known constitutive promoter, EF1α expression could not be visualized in sporozoites and the majority of male gametocytes. In the life stages that do show EF1α, there is considerable variation; oocysts were determined to have a very high level of transcript abundance while female gametocytes displayed significantly less (appendix 1b). HSP70-2/BiP on the other hand showed relatively consistent activity in all life stages. Therefore, this seems to indicate that the HSP70-2/BiP promoter is more reliable to use longitudinally within the parasites since it can more effectively drive consistent protein expression across the lifecycle with only a lapse in schizonts.

Similarly, six distinct promoters previously tested to be active at specific life stages of the malaria parasite [13,14,15,16], were tested for the purpose of determining if they truly were active only at these defined phases of the lifecycle. Experiments that rely upon stage specific (not stage

enriched) expression require well-defined promoters. For instance, if any of these promoter's activity was shown to be limited to only one stage of the parasite's lifecycle, then, using CRISPR/Cas9, parasites could be edited and genetically attenuated in preferred life cycle stages and could serve as the basis for a live attenuated parasite vaccine[5]. With this goal in mind, plasmids containing a GFP expression cassette driven by one of the six stage-specific promoters that are able to insert into the dispensable *p230p* genomic locus were created by Laura Bowman in her honors work. Transgenic parasites containing these six promoters were assayed using live fluorescence and IFAs at the various lifecycle stages of the parasite.

CLAG-A was the first promoter tested. It was originally described as an asexual-blood-stage promoter[16]; therefore, it was expected to be present solely in ring, trophozoite, and schizonts. Upon performing experiments, CLAG-A activity was seen in the asexual stages, as expected, but also within gametocytes, day-7 oocysts and the 48-hour liver stage suggesting that this promoter is not stage-specific. Proteomics data from *P. berghei* shows expression in male and female gametocytes[22], while RNAseq data also in *P. berghei* indicates expression in gametocytes[23] but at a lower level than the asexual stages. Similar transcriptomic data from *P. falciparum* indicates the presence of CLAG-A activity in gametocytes [24,25].

Dynein heavy chain delta (DD), a gene thought to be active only in male gametocytes, was then tested. Upon completion of the blood-stage IFAs it was apparent that DD was also not stage-specific. Expression was seen, in addition to male gametocytes, within rings and schizonts although to a lower extent. Although this precludes this promoter being used to create genetically-attenuated parasites, the fact that it is present only in male gametocytes means that it can be used for the purpose of separating male and female gametocytes[26]. IFAs performed on liver-stage parasites 24 hours post-feed revealed that no GFP expression occurred at this stage.

Following DD, the temporal activity of LAP4 was determined. LAP4 is defined as a female-specific promoter[16], however the blood-stage IFAs refuted this. Low levels of GFP expression were seen in all asexual stages and relatively similar expression was seen across both male and female gametocytes. In *P. falciparum*, there exists proteomic evidence for expression of LAP4 in all three asexual-blood stages as well as female and male gametocytes. Indicating that this promoter is likely active during the blood stages in general, but expression increases upon differentiation into male or female gametocytes[25, 27, 28].

The TRAP promoter activity was next determined. The TRAP promoter is described as a mosquito-stage promoter and is therefore expected to be present in oocysts as well as day-7 and 14 sporozoites. However, no expression was seen in day-7 oocysts, but rather activity was visualized to a low degree in male gametocytes and 42% of female gametocytes. That being said, Day-14 sporozoite IFAs indicate that TRAP is moderately active in this stage as GFP expression was distinguishable from background fluorescence. Transcriptomics data from *P. berghei* show TRAP promoter expression in asexual- and sexual-stage parasites[23, 25]. Similar data in *P. falciparum* also indicates that the TRAP promoter is active in all blood-stage parasites[24].

The temporal expression of the UIS4 promoter was likewise tested. Data from live fluorescence microscopy and IFAs revealed that this promoter, despite being expected to be active only in the late-mosquito stages and early-liver stage, was active at various blood-stages and in day-7 oocysts. Of the blood stages, low expression was seen in schizonts as well as male and female gametocytes. In Addition, day-10 sporozoites showed no expression while as expected, day-14 sporozoites displayed GFP expression but to a low degree as it did not seem to be much higher than background fluorescence. When the 24-hour liver stage IFAs were performed, the parasites showed very bright GFP fluorescence. This indicates that the parasite

begins to express the *uis4* mRNA in the salivary glands of mosquitoes and by 24 hours post-transmission to the host, the mRNA remains extremely abundant. Additionally, very low expression was seen in the 48-hour liver stage, however since this is described as an early-liver stage promoter, this expression may be due to residual proteins from the previous stage. Transcriptomics of *P. berghei* shows expression of UIS4 in the asexual-blood stages and gametocytes with the greatest level, among these 5 stages, occurring in schizonts[24, 25].

LISP2 was the final stage-specific promoter to be tested. This promoter was expected to be active in the 24- and 48-hour liver stages. However, the blood-stage IFAs demonstrated that this promoter is active to a small degree in female gametocytes. Other transcriptomic data from *P. berghei* suggests that this promoter is actually active throughout the blood stages, but very few transcripts are present[23, 25]. Additional *P. falciparum* transcriptomics experiments revealed that promoter is active to a very small, albeit equal, degree in male and female gametocytes[24] and low transcription levels are seen throughout all blood stages[28].

Recent single-cell RNAseq data, issued by the Wellcome Sanger Institute as the Malaria Cell Atlas, has provided an in-depth analysis of transcript abundance in individual cells at all stages of the malaria lifecycle (appendix 1c-h)[29]. This data differs in the transcriptomic information cited previously in that this provides specific details about transcription levels within each individual stage rather than as a gross representation of erythrocytic, early- and late-mosquito as well as liver stages. The Atlas ranks individual cells on a range from 0 to 15 with 0 being no detectable transcripts and 15 being in great abundance. The *P. berghei* orthologs of the stage-specific promoters tested in this study were used to determine relative transcription levels in individual cells.

According to the Atlas, CLAG-A transcripts can be detected to a great degree in rings, trophozoites and schizonts. A range of transcription levels can be seen in male gametocytes as well as within female gametocytes, which showed levels from. The female gametocyte data indicates a large variation in transcription among cells. Among oocysts, transcript levels were consistently low. Sporozoites show a varying degree of transcription as well; the majority of cells have no detectable transcripts. Liver stage cells showed expression levels very similar to the asexual erythrocytic stages (Appendix 1c).

DD is shown to be extremely abundant in male gametocytes, as is to be expected, with a score ~10. In all the other life stages, there is a constant, low transcript count. Although in most of the cells analyzed there are no detectable transcripts. This transcriptomics data is similar to the expression seen via the IFAs in this series of experiments. The only difference being that the Atlas shows low levels of transcripts throughout the stages, while the IFAs showed no significant expression. This could be due to the fact that since so few cells showed any levels of expression via RNAseq, other than male gametocytes, that there simply was not a great number of expressive cells in the population assayed using IFAs (Appendix 1d).

The Atlas shows a very large level of expression for LAP4 within female gametocytes (~10-12), which is expected since this was originally described as a female stage-specific promoter. However, in addition to female expression, a significant number of male gametocytes also show expression levels that are not greatly lower than female gametocytes (~3-10). Additionally, a small number of parasites in the other blood-stages as well as a few oocysts like was show expression. That being said, the number of cells with quantifiable expression is much fewer than those without it (Appendix 1e). This data is, therefore, consistent with the results of the various IFAs performed.

The single-cell-transcriptomics data for TRAP was then compared to the IFA results. TRAP is thought to be very active in mid-to-late-mosquito stages. The IFAs revealed that there was no expression in day-7 oocysts, but according to the transcriptomics, the gene is moderately active (~1-7). However, since the Atlas does not differentiate more specifically between the number of days post infection of the oocysts, it is likely that the oocysts displaying transcription are post day-7. This would be expected given the data suggesting it is active in later oocyst stages. This includes the day-10 IFAs performed in this work, which indicate active expression. The most active stage for this promoter according to the Atlas is sporozoites. This agrees well with the day 14 IFA data, which indicates moderate expression of GFP**.** Additionally, throughout the blood-stages moderate transcript levels are seen. In comparison to the RNAseq data, expression was only seen in male gametocytes and female gametocytes when visualized via IFA (Appendix 1f).

The Atlas indicates that UIS4 expression can be seen very strongly in sporozoites, which was the stage in which this promoter is expected to be active. Approximately half of the oocysts contained a moderate level of transcripts, which is consistent with the IFA data. Within each blood-stage very few cells with quantifiable transcript levels were seen, nonetheless this is likewise similar to the IFA results. In fact, there may have been a greater number of cells within the Sanger Institute's sample that actually contained transcripts, but due to the restrictions of RNAseq, were not able to be definitively quantified. Lastly, a large majority of liver stage parasites showed intermediate transcript levels. This and other data indicate that this promoter begins to become truly active in oocysts, transcript levels reach an all-time high in sporozoites, although translation is repressed, and then the number of transcripts is greatly reduced by the time the parasite enters the liver stages[30] (Appendix 1g).

The LISP2 promoter, according to the Atlas, is greatly active in the liver stage as was anticipated (~10-12). However, there is a considerable number of transcripts seen in oocysts, although the levels seen in these parasites are about half that seen in the liver stages. The asexual stages via the RNAseq data showed relatively high expression levels for rings, with expression of near 10 for some cells, and trophozoites, with a decent proportion showing expression of ~7. During the blood-stage IFAs a couple very dim schizonts, trophozoites, and female gametocytes were seen, but the majority appeared to be non-expressive. This might indicate that this promoter is very lightly active during the erythrocytic stages to the point that RNAseq was unable to detect a quantifiable number of transcripts (Appendix 1h).

The single-cell transcriptomics performed by the Sanger institute and the transcriptomics and proteomics cited previously in conjunction with the GFP expression assays that were performed in this work, provide an insight into the stage-specificity of these six promoters of interest. On several occasions the single-cell transcriptomics, which provides the most detailed account of these promoters' activity within individuals cells at specific stages, seem to contradict the IFA results and vice versa. However, it must be kept in mind that both of these assays have their restrictions. First, while the single-cell transcriptomics give a generally accurate indication of promoter activity, this depends on the criteria used to determine what qualifies as a valid read. Secondly, there is a minimum level of expression that must occur for RNAseq to be scored as present in the sample. Next, it is important to consider that while these promoters are ultimately derived from the parasite's own genome, they were taken out of their native context for the GFP expression assays that I conducted. Specifically, in creating the plasmids, anything upstream of the promoter was completely removed and the 3' UTR that would be present for that certain gene was replaced by that of the GFP coding sequence and an exogenous 3'UTR. These modifications

could have altered the true expression profile of these genes by effectively removing potential activator or inhibitor binding sites. It must be mentioned, however, that while these promoters were removed from their native context, they were placed into another that reflects how they could be used for transgene expression. Thus, the expression profiles seen in the IFAs are that which would be adhered to when using the promoters for the production of these transgenes. Furthermore, using GFP as a reporter to illustrate the relative level of expression of a gene can serve to exaggerate the true quantity of expression. This is because the half-life of GFP is far greater than that of mRNA, which causes more GFP to be quantitatively present than mRNA from which it was translated. Therefore, while it could be said that the IFAs performed do not offer a comprehensive explanation about the true expression of these genes in their genomic context, analyzing these various data sets together reveals valuable information for their use as a genetic tool.

That being said, when all of the proteomic, transcriptomic and IFA data are considered, it can be seen that none of the promoters originally thought to be stage-specific are active at only one particular stage of the lifecycle. Thus, while it is unlikely that any of these promoters could be used to create genetically-attenuated parasites that are “programmed” to become quiescent at a specific stage, there is some value it knowing that these promoters vary greatly in strength depending on the stage of life of the parasite. For example, DD, which has shown to be highly enriched in male gametocytes, although still present to a small degree in female gametocytes, or LAP4, which has shown the opposite expression characteristics, could be used to enact CRISPR modifications specifically in one type of gametocyte. In addition to this information, this work has provided an effective, reliable way of testing promoter activity using GFP expression paired with IFAs. Therefore, these assays could be manipulated in the future to characterize other

promoters of interest, especially when used in conjunction with reliable transcriptomic data such as that provided by the Malaria Cell Atlas.

In conclusion, this study sought to describe and characterize the activity of various promoters, both constitutive and stage specific, in the hopes of using them for a number of different applications, including the expression of CRISPR/Cas9 components. The constitutive promoter, BiP, was determined to be a suitable alternative to or could be used in conjunction with other constitutive promoters such as EF1α to drive Cas9 or RGR production. Additionally, the two lengths tested, 300bp and 500bp, showed that by altering the length of the promoter different levels of expression could be achieved. This disparity in expression levels could be due to the presence of activator binding site in the 500 bp construct that increases the relative promoter strength. For example, heat shock factors (HSF) and signal transducers and activators of transcription (STAT) have been previously described to alter transcription levels of HSP70[31]. Likewise, there are a myriad of well-characterized eukaryotic transcription factors that are known to be critical to the transcription mechanism and which bind regions up and downstream of the TATA box[32]. If any of these binding sites is disrupted, this could cause a decrease in transcription levels. Nevertheless, depending on the application and desired level of transcript production, the appropriate length promoter could be utilized. In terms of the stage-specific promoters, despite determining that the promoters tested in these experiments (CLAG-A, DD, LAP4, TRAP, UIS4 and LISP2) were in fact not active in only one specific stage of the parasite's lifecycle as previously thought, the expression trends of each promoter were able to be characterized and are described herein. With this information, the utility of certain promoters to drive CRISPR-component production to enact gene deletions, replacement or a number of other applications within specific stages was determined. Furthermore, a method for determining the

activity of a promoter-of-interest was pioneered within *P. yoelii* using engineered plasmids containing GFP driven by a specific promoter and visualized via IFAs at multiple lifecycle stages.

Future Directions

One of the strengths of this method is that it can be adapted for use with any promoter-of-interest. Thus, in the future, if another promoter is suspected to be stage-specific, this method provides a way to validate this. The one downfall of this method is that it does not take into account that the lack of GFP expression could be due to transcriptional or translational repression. Therefore, this is best used as supporting evidence alongside transcriptomic and proteomic data. Furthermore, upon determining that the HSP70-2/BiP promoter is effective at constitutively driving expression *in vivo,* it is evident that the constitutive and stage-specific promoter experiments are complementary. The HSP70-2/BiP promoter, along with another constitutive promoter (e.g. EF1α), could be used to drive Cas9 and RGR production such that they enact a modification to a gene. If the modified gene is suspected to be stage-specific, the GFP-expression plasmid can be modified such that the promoter of this gene drives GFP expression. Its expression can be visualized via live fluorescence and immunofluorescence assay providing information about the gene's expression patterns.

Further expansion and application of this method could include characterizing transcriptional and translational repressors and activators as well as be used to determine if a transcriptional or translational regulator could be used to control stage-specific expression. For example, our lab has previously shown that ALBA4 is a predicted translational regulator in the parasite's transmission stages[33]. Therefore, if its *cis*-regulatory region could be inserted upstream of the GFP-coding sequence and whose transcription is driven by a constitutive promoter like

BiP or EF1α, the stage-specific effects of this regulator could be characterized. This would then provide an alternative means to produce genetically attenuated parasites rather than relying on a promoter with inherent temporally regulated properties.

Year after year hundreds of thousands of individuals die of malaria, therefore a safe, reliable and effective method for the treatment of the parasite remains a top priority within developing countries across the globe. Recent scientific advancement has pinpointed CRISPR/Cas9 as a promising method for creating genetically altered parasites that could be used to create a vaccine. With this in mind, this work sought to determine the plausibility of using one of six stage-specific promoters to create transgenic parasites that are "programmed" to become incapable of maturing further upon activation of the promoter in a certain life stage. And, ultimately, while these promoters were determined to be improper candidates for this application, the method by which this was determined serves as a prototype that can be improved upon and applied further within *Plasmodium*.

Appendix 1

Malaria Cell Atlas Data

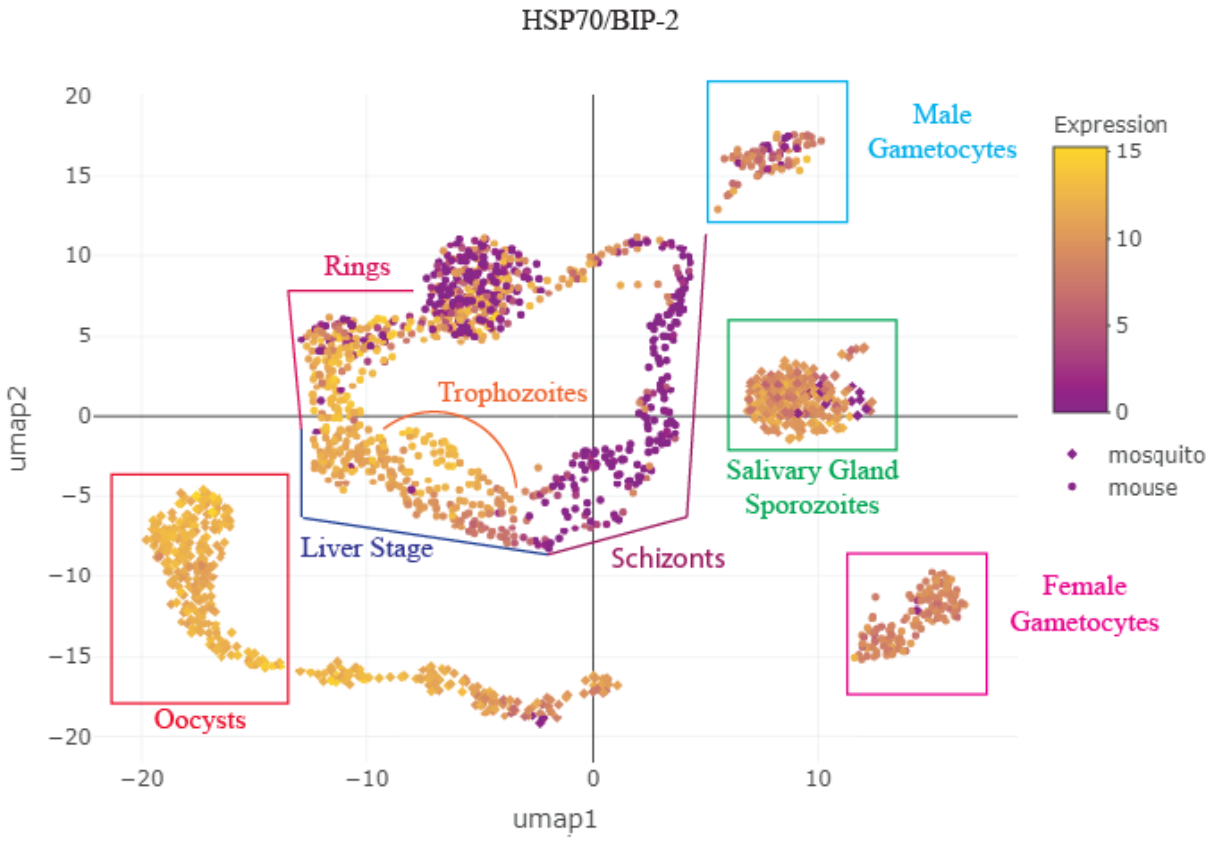

Appendix 1a. HSP70-2/BiP Malaria Cell Atlas. Relative transcript abundance from 0-15 for *P. berghei* HSP70-2/BiP (PBANKA_0711900) in individual lifecycle stages. Axes indicate pseudotime, which was measured by fitting an ellipse to the data and calculating the angle (radians) around the center of this ellipse for each cell relative to the start cell. These data were collected from the Wellcome Sanger Institute's Malaria Cell Atlas (https://www.sanger.ac.uk/science/tools/mca/mca/) and modified using Adobe Illustrator to denote in which stage of development the parasites are.

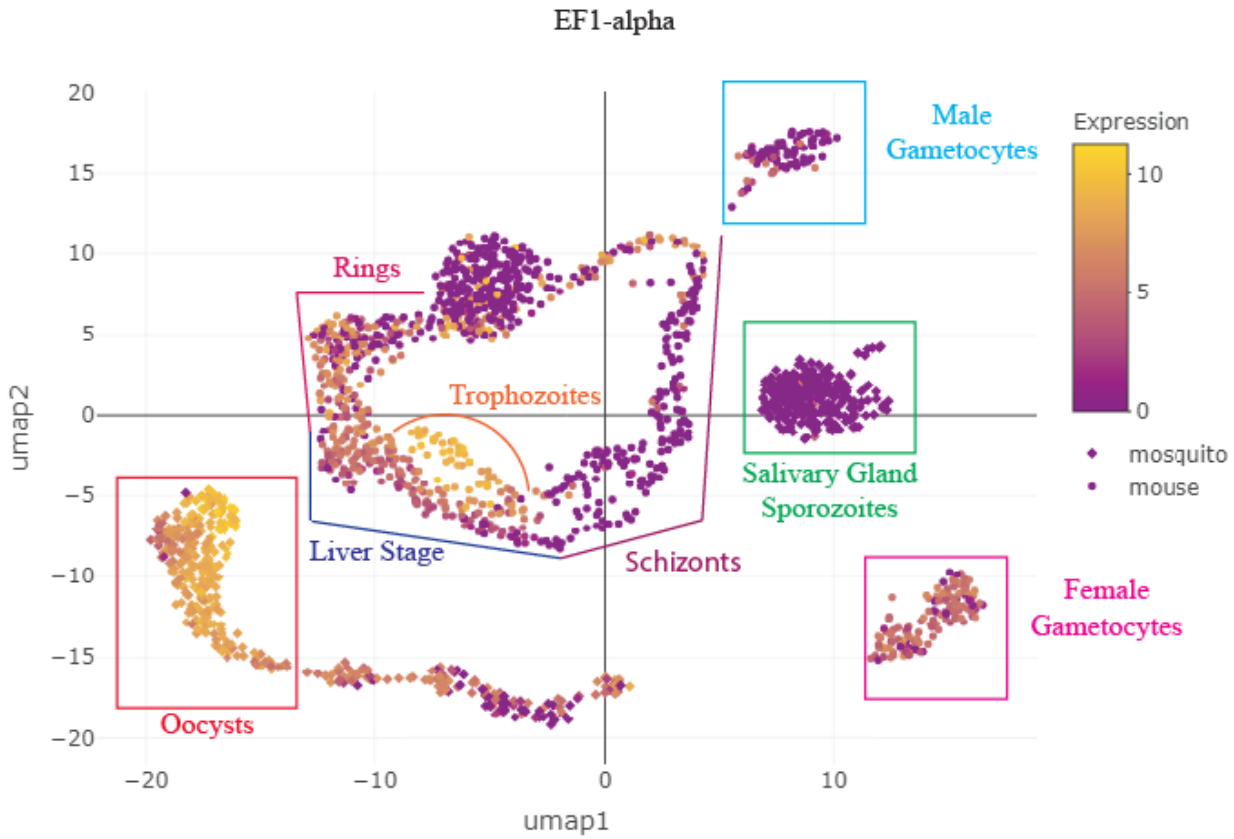

Appendix 1b. EF1α Malaria Cell Atlas. Relative transcript abundance from 0-15 for *P. berghei* **EF1α** (PBANKA_1133400) in individual lifecycle stages. Axes indicate pseudotime, which was measured by fitting an ellipse to the data and calculating the angle (radians) around the center of this ellipse for each cell relative to the start cell. These data were collected from the Wellcome Sanger Institute's Malaria Cell Atlas (https://www.sanger.ac.uk/science/tools/mca/mca/) and modified using Adobe Illustrator to denote in which stage of development the parasites are.

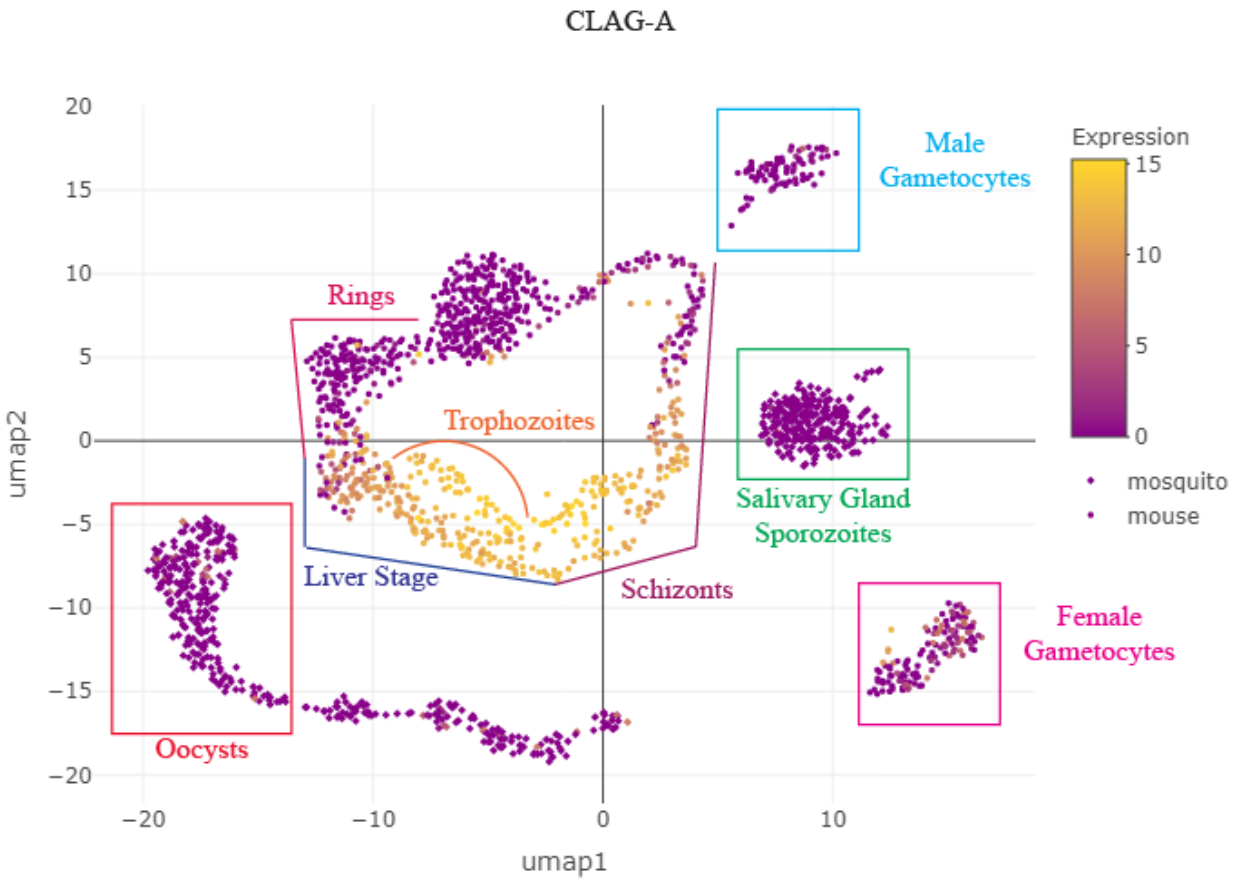

Appendix 1c. CLAG-A Malaria Cell Atlas. Relative transcript abundance from 0-15 for *P. berghei* CLAG-A (PBANKA_1400600) in individual lifecycle stages. Axes indicate pseudotime, which was measured by fitting an ellipse to the data and calculating the angle (radians) around the center of this ellipse for each cell relative to the start cell. These data were collected from the Wellcome Sanger Institute's Malaria Cell Atlas (https://www.sanger.ac.uk/science/tools/mca/mca/) and modified using Adobe Illustrator to denote in which stage of development the parasites are.

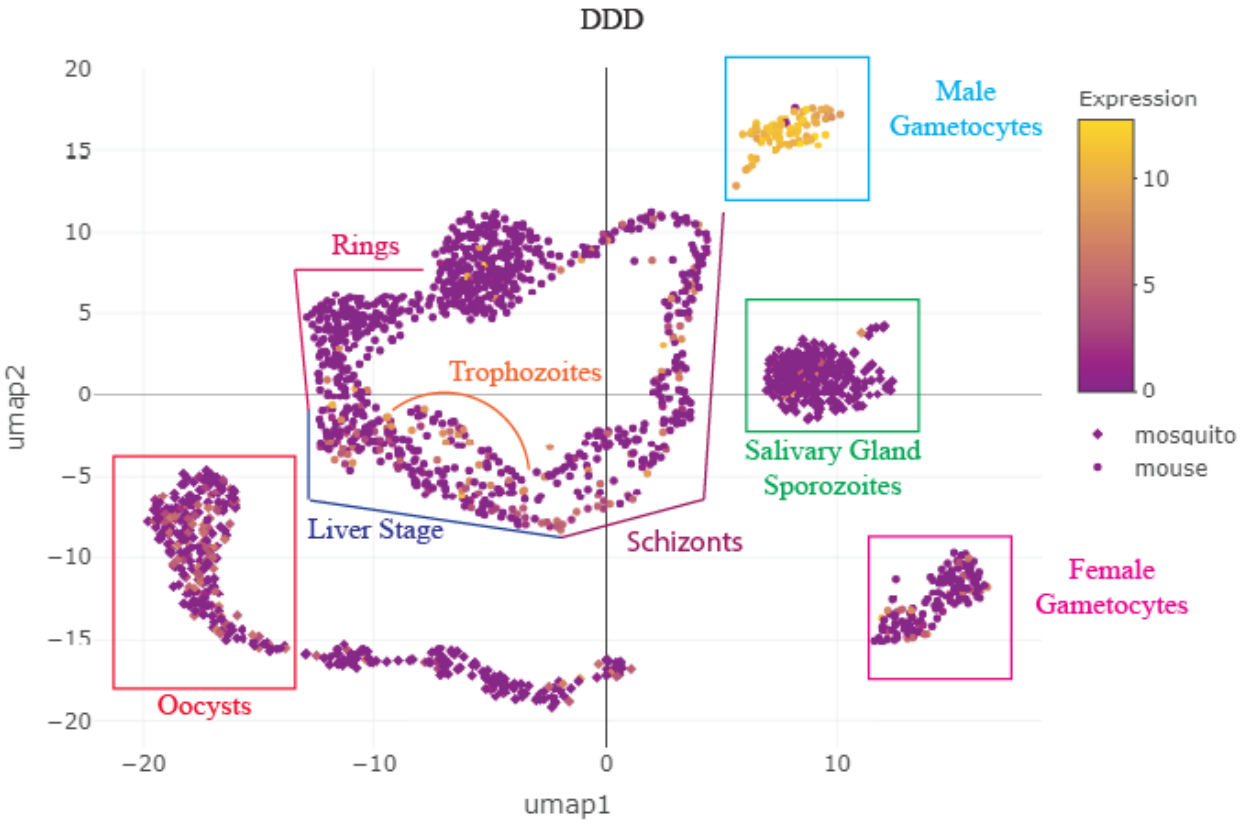

Appendix 1d. DD Malaria Cell Atlas. Relative transcript abundance from 0-15 for *P. berghei* DD (PBANKA_0416100) in individual lifecycle stages. Axes indicate pseudotime, which was measured by fitting an ellipse to the data and calculating the angle (radians) around the center of this ellipse for each cell relative to the start cell. These data were collected from the Wellcome Sanger Institute's Malaria Cell Atlas (https://www.sanger.ac.uk/science/tools/mca/mca/) and modified using Adobe Illustrator to denote in which stage of development the parasites are.

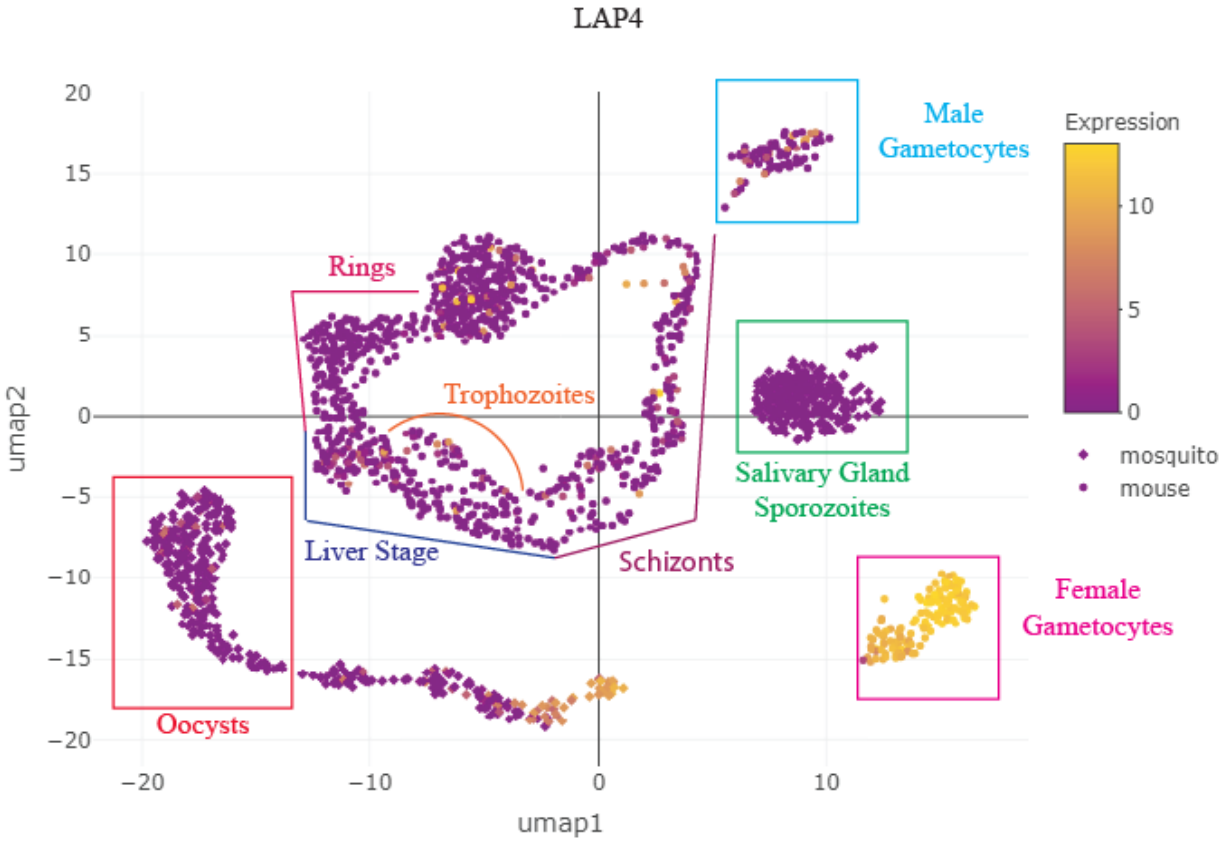

Appendix 1e. LAP4 Malaria Cell Atlas. Relative transcript abundance from 0-15 for *P. berghei* LAP4 (PBANKA_1319500) in individual lifecycle stages. Axes indicate pseudotime, which was measured by fitting an ellipse to the data and calculating the angle (radians) around the center of this ellipse for each cell relative to the start cell. These data were collected from the Wellcome Sanger Institute's Malaria Cell Atlas (https://www.sanger.ac.uk/science/tools/mca/mca/) and modified using Adobe Illustrator to denote in which stage of development the parasites are.

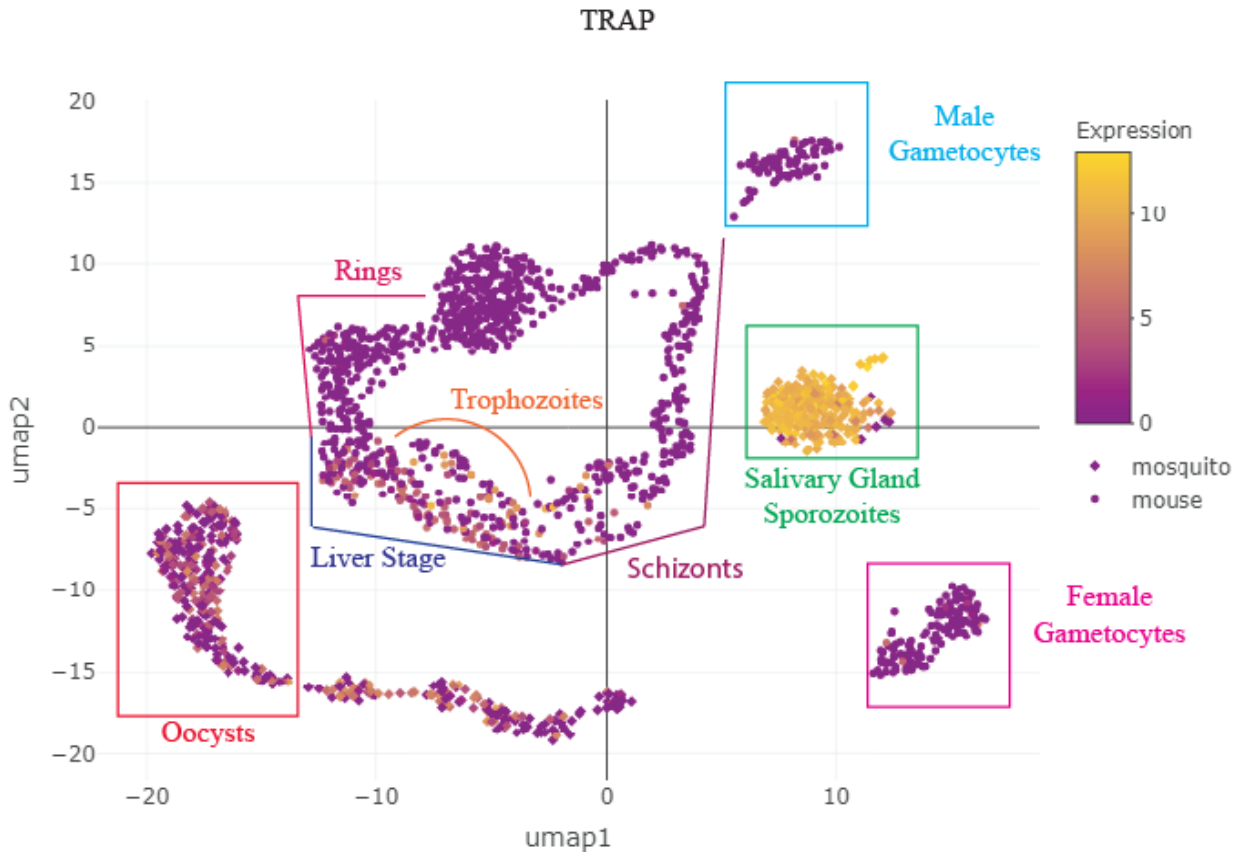

Appendix 1f. TRAP Malaria Cell Atlas. Relative transcript abundance from 0-15 for *P. berghei* TRAP (PBANKA_1349800) in individual lifecycle stages. Axes indicate pseudotime, which was measured by fitting an ellipse to the data and calculating the angle (radians) around the center of this ellipse for each cell relative to the start cell. These data were collected from the Wellcome Sanger Institute's Malaria Cell Atlas (https://www.sanger.ac.uk/science/tools/mca/mca/) and modified using Adobe Illustrator to denote in which stage of development the parasites are.

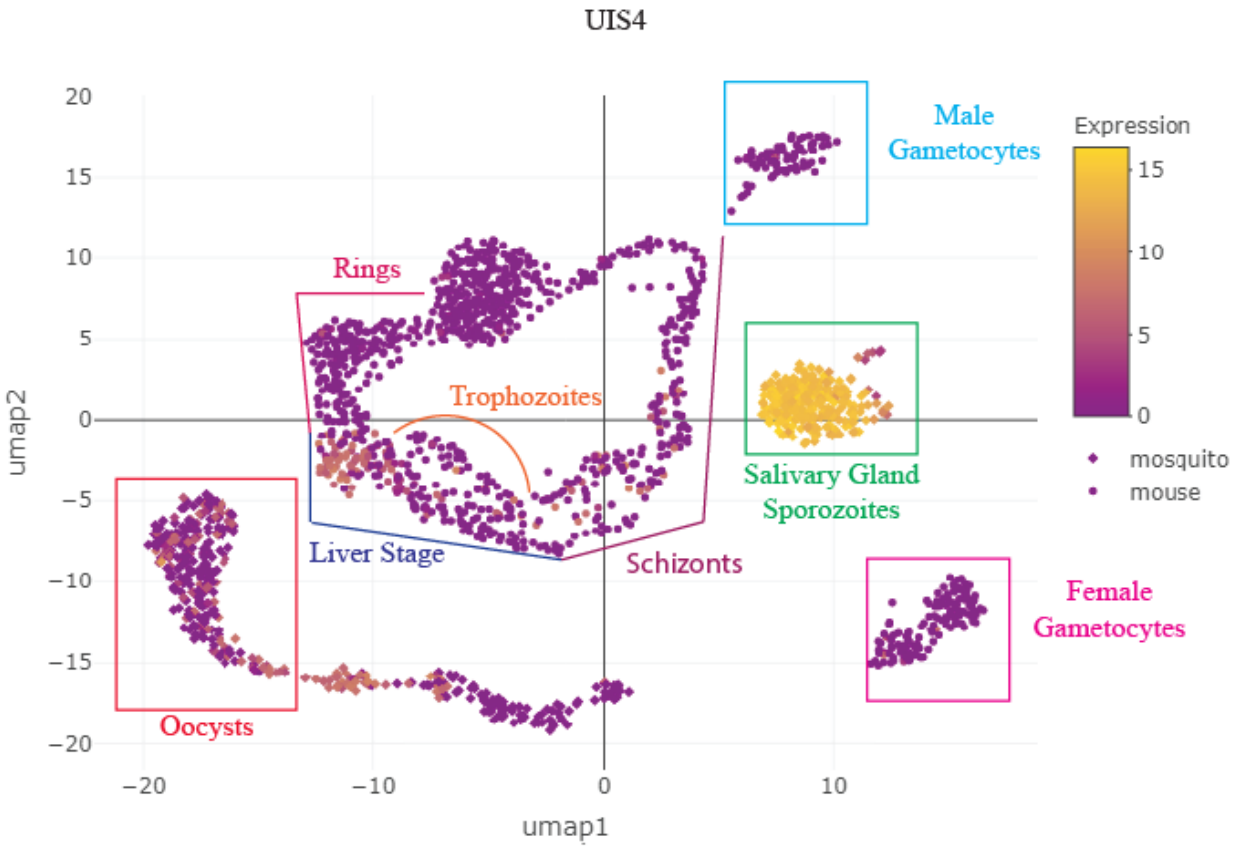

Appendix 1g. UIS4 Malaria Cell Atlas. Relative transcript abundance from 0-15 for *P. berghei* UIS4 (PBANKA_0501200) in individual lifecycle stages. Axes indicate pseudotime, which was measured by fitting an ellipse to the data and calculating the angle (radians) around the center of this ellipse for each cell relative to the start cell. These data were collected from the Wellcome Sanger Institute's Malaria Cell Atlas (https://www.sanger.ac.uk/science/tools/mca/mca/) and modified using Adobe Illustrator to denote in which stage of development the parasites are.

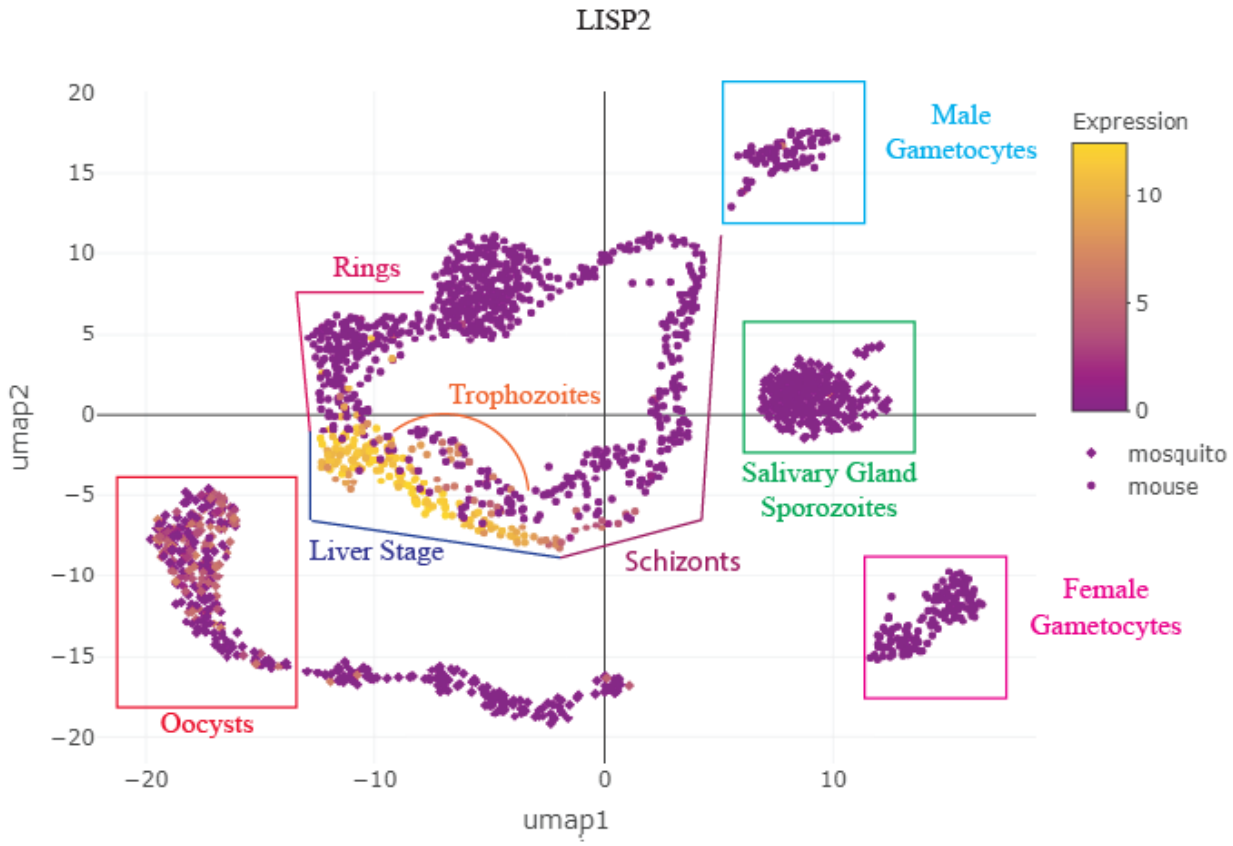

Appendix 1h. LISP2 Malaria Cell Atlas. Relative transcript abundance from 0-15 for *P. berghei* LISP2 (PBANKA_1003000) in individual lifecycle stages. Axes indicate pseudotime, which was measured by fitting an ellipse to the data and calculating the angle (radians) around the center of this ellipse for each cell relative to the start cell. These data were collected from the Wellcome Sanger Institute's Malaria Cell Atlas (https://www.sanger.ac.uk/science/tools/mca/mca/) and modified using Adobe Illustrator to denote in which stage of development the parasites are.

Appendix 2

Appendix 2a. Oligonucleotides Used for Cloning

Construct	Description	Oligonucleotide (5'-3')
	Creation of Recombinant Sequence	
300 bp HSP70-2/BiP Promoter (pSL1190)	FWD	CAGCGGCCGCGCATAGAAGAATTCATACATTGTGCTTAAAAAGAAATATTTAAG
	REV	GCGCTAGCCATTTGCTTTAATTTTTATGCATACAAAATTAATTAATAAAAATAATAATGTAATTAATTCTTGTTC
500 bp HSP70-2/BiP Promoter (pSL1196)	FWD	CAGCGGCCGCGCATATTATATCACATATTTTATGAATGTGCATAATATTTATTGCTTGTT
	REV	GCGCTAGCCATTTGCTTTAATTTTTATGCATACAAAATTAATTAATAAAAATAATAATGTAATTAATTCTTGTTC
	Genotyping PCR	
300 bp HSP70-2/BiP Promoter (pSL1190)	5' External	CTCCATCCTCATATGGTTTAATCATACTCAAATATCTTTTTAGTAGTTCCTC
	3' External	GTAATTGGAATCAAATTAGAAGGATATGAATTAGATCCACCAAATTG
	5' Internal	CCGTATGTTGCATCACCTTCACCCTCTCCACTGACAG
	3' Internal	CCAGGAGGAGAAAGGCATTAAGTACAAATTTGAAGTATATGAGAAG
500 bp HSP70-2/BiP Promoter (pSL1196)	5' External	CTCCATCCTCATATGGTTTAATCATACTCAAATATCTTTTTAGTAGTTCCTC
	3' External	GTAATTGGAATCAAATTAGAAGGATATGAATTAGATCCACCAAATTG
	5' Internal	CCGTATGTTGCATCACCTTCACCCTCTCCACTGACAG
	3' Internal	CCAGGAGGAGAAAGGCATTAAGTACAAATTTGAAGTATATGAGAAG

Appendix 2b. *P. yoelii* and *P. berghei* Gene IDs associated with Constitutive and Stage-Specific Promoters

Gene ID (*P. yoelii*)	Gene ID (*P. berghei*)	Promoter
PY17X_0712100	PBANKA_0711900	HSP70-2/BiP (1090 & 1096)
PY17X_1402200	PBANKA_1400600	CLAG-A (1019)
PY17X_0418900	PBANKA_0416100	DD (1020)
PY17X_1323300	PBANKA_1319500	LAP4 (1018)
PY17X_1354800	PBANKA_1349800	TRAP (1082)
PY17X_0502200	PBANKA_0501200	UIS4 (1083)
PY17X_1004400	PBANKA_1003000	LISP2 (1017)

Bibliography

1. "WHO | Malaria World Report 2018." WHO. Accessed February 22, 2019. https://www.who.int/malaria/publications/world-malaria-report-2018/report/en/
2. "Efficacy and Safety of RTS,S/AS01 Malaria Vaccine with or without a Booster Dose in Infants and Children in Africa: Final Results of a Phase 3, Individually Randomised, Controlled Trial." *The Lancet* 386, no. 9988 (July 2015): 31–45.
3. "RTS,S." PATH's Malaria Vaccine Initiative, September 15, 2015. https://www.malariavaccine.org/malaria-and-vaccines/first-generation-vaccine/rtss.
4. Cowman, Alan F., Julie Healer, Danushka Marapana, and Kevin Marsh. "Malaria: Biology and Disease." *Cell* 167, no. 3 (October 2016): 610–24.
5. Annoura, Takeshi, Ivo H. J. Ploemen, Ben C. L. van Schaijk, Mohammed Sajid, Martijn W. Vos, Geert-Jan van Gemert, Severine Chevalley-Maurel, et al. "Assessing the Adequacy of Attenuation of Genetically Modified Malaria Parasite Vaccine Candidates." *Vaccine* 30, no. 16 (March 30, 2012): 2662–70.
6. Mali, P., Aach, J., Stranges, P. B., Esvelt, K. M., Moosburner, M., Kosuri, S., Church, G. M. (2013). CAS9 transcriptional activators for target specificity screening and paired nickases for cooperative genome engineering. Nat Biotechnol Nature Biotechnology, 31 (9), 833-838
7. Lee, Andrew H., Lorraine S. Symington, and David A. Fidock. "DNA Repair Mechanisms and Their Biological Roles in the Malaria Parasite Plasmodium Falciparum." *Microbiol. Mol. Biol. Rev.* 78, no. 3 (September 1, 2014): 469–86.
8. Gao, Y., & Zhao, Y. (2014). Self-processing of ribozyme-flanked RNAs into guide RNAs in vitro and in vivo for CRISPR-mediated genome editing. Journal of Integrative Plant Biology J. Integr. Plant Biol., 56 (4), 343-349.
9. Walker, Michael P., and Scott E. Lindner. "Ribozyme-Mediated, Multiplex CRISPR Gene Editing and CRISPRi in Plasmodium Yoelii." *BioRxiv*, November 29, 2018, 481416.
10. Zhang W-W, Matlashewski G. 2015. CRISPR-Cas9-Mediated Genome Editing in Leishmania donovani. mBio 6. 29.
11. Lee RTH, Ng ASM, Ingham PW. 2016. Ribozyme Mediated gRNA Generation for In Vitro and In Vivo CRISPR/Cas9 Mutagenesis. PLOS ONE 11:e0166020.
12. Sebastian, S., Brochet, M., Collins, M., Schwach, F., Jones, M., Goulding, D., Billker, O. (2012). A Plasmodium Calcium-Dependent Protein Kinase Controls Zygote Development and Transmission by Translationally Activating Repressed mRNAs. Cell Host & Microbe,12 (1), 9-19.
13. "RMgmDB - Rodent Malaria Genetically Modified Parasites - P. Berghei." RMgmDB Rodent Malaria Genetically Modified Parasites - P. Berghei. Leiden University Malaria Research Group, 18 Feb. 2009. Web. 14 Mar. 2017.
14. Eksi S, Suri A, Williamson KC. Sex and stage-specific reporter gene expression in Plasmodium falciparum. Molecular and biochemical parasitology. 2008;160(2):148-151.
15. Singer, M., Marshall, J., Heiss, K., Mair, G. R., Grimm, D., Mueller, A., & Frischknecht, F. (2015). Zinc finger nuclease-based double-strand breaks attenuate malaria parasites and reveal rare microhomology-mediated end joining. Genome Biology, 16 (1).

16. Niz, M. D., Helm, S., Horstmann, S., Annoura, T., Portillo, H. A., Khan, S. M., & Heussler, V. T. (2015). In Vivo and In Vitro Characterization of a Plasmodium Liver Stage-Specific Promoter. *PLOS ONE PLoS ONE, 10*(4).
17. Radons, Jürgen. "The Human HSP70 Family of Chaperones: Where Do We Stand?" *Cell Stress & Chaperones* 21, no. 3 (May 2016): 379–404.
18. Bowman, L. (2017). "Identification and Validation of Crispr/Cas9 Stage-Specific Promoters and An Alternative Fluorescent Reporter to GFP for *Plasmodium Yoelii*," (unpublished undergraduate honors thesis). Retrieved from https://honors.libraries.psu.edu/catalog
19. Janse C., Ramesar J., Waters A. (2006). High-efficiency transfection and drug selection of genetically transformed blood stages of the rodent malaria parasite *Plasmodium berghei. Natural Protocols. 1(10),* 346-356.
20. Dijk, Melissa R. van, Ben C. L. van Schaijk, Shahid M. Khan, Maaike W. van Dooren, Jai Ramesar, Szymon Kaczanowski, Geert-Jan van Gemert, et al. "Three Members of the 6-Cys Protein Family of Plasmodium Play a Role in Gamete Fertility." *PLoS Pathogens* 6, no. 4 (April 8, 2010)
21. Sebastian, S., Brochet, M., Collins, M., Schwach, F., Jones, M., Goulding, D., . . . Billker, O. (2012). A Plasmodium Calcium-Dependent Protein Kinase Controls Zygote Development and Transmission by Translationally Activating Repressed mRNAs. *Cell Host & Microbe, 12*(1), 9-19.
22. Mair, Gunnar R., Edwin Lasonder, Lindsey S. Garver, Blandine M. D. Franke-Fayard, Céline K. Carret, Joop C. A. G. Wiegant, Roeland W. Dirks, George Dimopoulos, Chris J. Janse, and Andrew P. Waters. "Universal Features of Post-Transcriptional Gene Regulation Are Critical for Plasmodium Zygote Development." *PLoS Pathogens* 6, no. 2 (February 12, 2010)
23. Yeoh, Lee M., Christopher D. Goodman, Vanessa Mollard, Geoffrey I. McFadden, and Stuart A. Ralph. "Comparative Transcriptomics of Female and Male Gametocytes in Plasmodium Berghei and the Evolution of Sex in Alveolates." *BMC Genomics* 18 (September 18, 2017).
24. Lasonder, Edwin, Sanna R. Rijpma, Ben C. L. van Schaijk, Wieteke A. M. Hoeijmakers, Philip R. Kensche, Mark S. Gresnigt, Annet Italiaander, et al. "Integrated Transcriptomic and Proteomic Analyses of P. Falciparum Gametocytes: Molecular Insight into Sex-Specific Processes and Translational Repression." *Nucleic Acids Research* 44, no. 13 (27 2016): 6087–6101.
25. Otto, Thomas D., Daniel Wilinski, Sammy Assefa, Thomas M. Keane, Louis R. Sarry, Ulrike Böhme, Jacob Lemieux, et al. "New Insights into the Blood-Stage Transcriptome of Plasmodium Falciparum Using RNA-Seq." *Molecular Microbiology* 76, no. 1 (April 2010): 12–24.
26. Hart, Kevin J., Jenna Oberstaller, Michael P. Walker, Allen M. Minns, Mark F. Kennedy, Ian Padykula, John H. Adams, and Scott E. Lindner. "Plasmodium Male Gametocyte Development and Transmission Are Critically Regulated by the Two Putative Deadenylases of the CAF1/CCR4/NOT Complex." *PLOS Pathogens* 15, no. 1 (January 31, 2019)
27. López-Barragán, María J., Jacob Lemieux, Mariam Quiñones, Kim C. Williamson, Alvaro Molina-Cruz, Kairong Cui, Carolina Barillas-Mury, Keji Zhao, and Xin-zhuan Su. "Directional Gene Expression and Antisense Transcripts in Sexual and Asexual Stages of Plasmodium Falciparum." *BMC Genomics* 12, no. 1 (November 30, 2011): 587.

28. Painter, Heather J., Manuela Carrasquilla, and Manuel Llinás. “Capturing in Vivo RNA Transcriptional Dynamics from the Malaria Parasite Plasmodium Falciparum.” *Genome Research* 27, no. 6 (2017): 1074–86
29. Howick, Virginia M., Andrew Russell, Tallulah Andrews, Haynes Heaton, Adam J. Reid, Kedar Nath Natarajan, Hellen Butungi, et al. “The Malaria Cell Atlas: A Comprehensive Reference of Single Parasite Transcriptomes across the Complete Plasmodium Life Cycle.” *BioRxiv*, January 22, 2019, 527556.
30. Silva, Patrícia A. G. C., Ana Guerreiro, Jorge M. Santos, Joanna A. M. Braks, Chris J. Janse, and Gunnar R. Mair. “Translational Control of UIS4 Protein of the Host-Parasite Interface Is Mediated by the RNA Binding Protein Puf2 in Plasmodium Berghei Sporozoites.” *PLOS ONE* 11, no. 1 (January 25, 2016)
31. Stephanou, A, Latchman, D.S. “Transcriptional Regulation of the Heat Shock Protein Genes by STAT Family Transcription Factors.”; Gene Expr. 7(4-5-6) (1999): 311–319.
32. Yang, Vincent W. “Eukaryotic Transcription Factors: Identification, Characterization and Functions.” *The Journal of Nutrition* 128, no. 11 (November 1, 1998): 2045–51.
33. Muñoz, Elyse E., Kevin J. Hart, Michael P. Walker, Mark F. Kennedy, Mackenzie M. Shipley, and Scott E. Lindner. “ALBA4 Modulates Its Stage-Specific Interactions and Specific MRNA Fates during Plasmodium Growth and Transmission.” *Molecular Microbiology* 106, no. 2 (October 2017): 266–84.

Academic Vita

LOGAN E FINGER
ljf5165@psu.edu

EDUCATION

The Pennsylvania State University **2019**
Major: Bachelor of Science in Biochemistry and Molecular Biology
Minor: Italian Language
Thesis: "*Defining Stage-Specific and Constitutive Promoters in Plasmodium yoelii"*

AWARDS

Schreyer Honors College Scholar	**2015-Present**
Academic Excellence Scholarship	**2015-Present**
Dandrea Trustee Scholarship	**2015-2017**
President's Freshman Award	**2015**
Dean's List (8x)	**2015-Present**
Bright Life Sciences Scholarship Recipient	**2017-2018**
Lewis and Opal D. Gugliemelli Honors Scholarship	**2018-2019**
Evan Pugh Scholar Senior Award Recipient	**2018**

TEACHING EXPERIENCE

Learning Assistant for BMB 398B, Introductory Molecular and Cell Biology,

The Pennsylvania State University

8/2017 – 5/2018

I, in addition to two other peers, led a weekly application-based course that is an extension of a concurrent molecular and cell biology class where we enhance students' knowledge of the biochemical concepts covered in the concurrent course.

Italian Tutor, The Pennsylvania State University

4/2016 – Present

As a tutor, I am responsible for leading group help sessions by assisting students in the areas of the language in which they are struggling. This is most often done by designing study guides and creating questions with the intention of strengthening students' skills.

RESEARCH

Lindner Lab, The Pennsylvania State University

8/2017 – Present

I am conducting research on promoters that allow for protein expression at certain points in the malaria parasite's life cycle. Visualization of protein expression via fluorescence microscopy will help to determine the viability of these promoters as a candidate for driving expression of CRISPR components. The presence of these fluorescence proteins will be monitored at several different time stages within the life cycle of the parasite within the mosquitoes and mice. With the knowledge gained from this work we will be able to target essential genes in the mosquito for potential use as a genetically attenuated parasite vaccine.

Showalter Lab, The Pennsylvania State University

1/2016 – 1/2017

I was studying the intrinsically disorder C-terminal domain of eukaryotic RNA Polymerase II. We performed experiments with the hopes of isolating protein factors that interact with the domain based upon the local allosteric changes that occur due to phosphorylation and the replacement of amino acids in the consensus sequence.

Pennsylvania Governor School for The Sciences,

Carnegie Mellon University
6/2014-8/2014
I was one of sixty rising seniors from across Pennsylvania selected for this program, which exposed us to a myriad of college-level courses, which encompassed many different disciplines within the field of science. Additionally, we worked in teams to complete a research project, which culminated in a publication in the school's personal journal.

PUBLICATIONS AND PAPERS

"A Study of High Temperature Superconductivity with Chemical Substitutions in the 123 and 2223 Systems"
Austin, Josiah, Catalano Renee, Finger, Logan, Haag Robert, Huffman Noah, Keebler, Timothy, Kratzer, Madison

The PGSS Journal, Vol. 29

http://www.pgssalumni.org/the-pgss-journal **2014**

CLINICAL EXPERIENCE

Shadowing/Observing

As an observer, I was privileged to be able to shadow doctors both within an operating room and office setting. I was able to experience medical procedures and direct patient contact in a variety of disciplines and specialties. I spent a total of ~50 hours shadowing physicians in orthopedic surgery, cardio electrophysiology, interventional cardiology, and emergency medicine.

- ~16 hours of surgery and office visits with Dr. Armando Avolio
- ~16 hours of heart catherization lab and office experience with Drs. Leonard Ganz, William Slemenda, and Christopher Morgan
- ~ 16 hours of emergency medicine experience with Drs. Kyle Kutrovac, Joseph Montibeller and Jacqueline Roth

LEADERSHIP

Swing Dance Club Treasurer, The Pennsylvania State University

8/2018-Present

Manage finances, seek fundraising opportunities and secure funding for Swing Dance Club meetings and events that include, but are not limited to, dance workshops, exchanges and travel events.

Newman Catholic Student Association IM Sports Coordinator, The Pennsylvania State University

8/2018-Present

Organize men's, women's and co-ed sports teams to compete on an intramural level in variety of sports such as soccer, football, ultimate frisbee, etc. Additionally, as an executive board member I am responsible for serving as one of the representatives for the active club members and for planning and leading general body meetings.

Chemistry Department Grader, The Pennsylvania State University

1/2018-Present

Grade homework and exams for CHEM 210 (Organic Chemistry I), CHEM 212 (Organic Chemistry II), and CHEM 310 (Introductory Inorganic Chemistry).

Swing Dance Instructor, Swing Dance Club at The Pennsylvania State University

8/2017 – Present

Teach beginner and intermediate lessons in Lindy Hop during bi-weekly club meetings and monthly public social dances.

ADDITIONAL SKILLS

- Near native proficiency in reading, writing and speaking Italian

- Knowledge of basic laboratory skills associated with generating recombinant DNA
- Experience creating transgenic organisms via transfection
- Ability to isolate, purify and characterize protein via column chromatography, dialysis, centrifugation, crystallization, etc.
- Experience with various types of mouse methodologies such as tail snips, tail-vein injections, cardiac punctures and liver dissection
- Familiarity with performing immunofluorescence assays and using fluorescence microscopy
- Experience with mosquito midgut and salivary gland dissections
- Proficiency in Microsoft Office and Adobe Illustrator
- Basic knowledge of Minitab statistical software